Award Number: DAMD17-00-1-0468

TITLE: Measurement of the Electron Density Distribution of Estrogens - A First Step to Advanced Drug Design

PRINCIPAL INVESTIGATOR: Damon A. Parrish
A. Alan Pinkerton, Ph.D.

CONTRACTING ORGANIZATION: University of Toledo
Toledo, Ohio 43606-3390

REPORT DATE: July 2003

TYPE OF REPORT: Annual Summary

PREPARED FOR: U.S. Army Medical Research and Materiel Command
Fort Detrick, Maryland 21702-5012

REPORT DOCUMENTATION PAGE

Form Approved
OMB No. 074-0188

1. AGENCY USE ONLY (Leave blank)	2. REPORT DATE	3. REPORT TYPE AND DATES COVERED
	July 2003	Annual Summary (15 Jul 00 - 14 Jun 03)

4. TITLE AND SUBTITLE
Measurement of the Electron Density Distribution of Estrogens - A First Step to Advanced Drug Design

5. FUNDING NUMBERS
DAMD17-00-1-0468

6. AUTHOR(S)
Damon A. Parrish
A. Alan Pinkerton, Ph.D.

7. PERFORMING ORGANIZATION NAME(S) AND ADDRESS(ES)
University of Toledo
Toledo, Ohio 43606-3390

E-Mail: Dparris2@uoft02.utoledo.edu

8. PERFORMING ORGANIZATION REPORT NUMBER

9. SPONSORING / MONITORING AGENCY NAME(S) AND ADDRESS(ES)
U.S. Army Medical Research and Materiel Command
Fort Detrick, Maryland 21702-5012

10. SPONSORING / MONITORING AGENCY REPORT NUMBER

11. SUPPLEMENTARY NOTES
Original contains color plates: All DTIC reproductions will be in black and white.

12a. DISTRIBUTION / AVAILABILITY STATEMENT
Approved for Public Release; Distribution Unlimited

12b. DISTRIBUTION CODE

13. ABSTRACT (Maximum 200 Words)

It has been shown that the development of certain types of cancer can be hormone dependent. Estrogens, such as estradiol, have the ability to bind as ligands to the estrogen receptor in the first of many steps which could result in the activation or repression of genes critical in the mechanism of tumor growth. The principle objective of this proposal is to relate known biological reactions to physical properties such as point charges of atoms and the electrostatic potential.

We are obtaining information about these electronic properties of estrogen derivatives from experimental determination of their electron density using high quality single crystal X-ray crystallography. During the past year, the focus was in completing Task 3, analysis of charge density data sets, for three systems (17β-estradiol•½MeOH, 17αestradiol•½H_2O, and 17α-estradiol•urea). Data integration techniques have been refined to improve overall data quality and consistency. Topological analysis has been completed, while analysis of the electrostatic potential is nearly complete. Initial comparisons have yielded some expected and unexpected results. These will be discussed in the body of the report. Continued effort must be made to obtain more quality data of different systems to increase the amount of data we have to reference to.

14. SUBJECT TERMS
Breast Cancer, X-ray Crystallography, Estrogens, Drug Design

15. NUMBER OF PAGES
54

16. PRICE CODE

17. SECURITY CLASSIFICATION OF REPORT	18. SECURITY CLASSIFICATION OF THIS PAGE	19. SECURITY CLASSIFICATION OF ABSTRACT	20. LIMITATION OF ABSTRACT
Unclassified	Unclassified	Unclassified	Unlimited

Table of Contents

Introduction

It has been shown that the development of certain types of cancer can be hormone dependent. Estrogens, such as estradiol, have the ability to bind as ligands to the estrogen receptor in the first of many steps which could result in the activation (agonistic effect) or repression (antagonistic effect) of genes critical in the mechanism of tumor growth. It is the object of this study to relate physical and chemical properties of estrogen derivatives to certain observed biological functions. It is hoped that detailed analysis of X-ray crystallographic data will provide important information to assist in the development of therapeutic drugs. My role is the experimental determination of the electron density distribution of several estrogens as part of a larger study to investigate a wide variety of estrogens.

Body

Task 1. Preliminary studies on a series of crystals of 'A- and D-ring' estrogen derivatives.

- Develop crystallization methods for the derivatives which are not yet available as charge density quality single crystals.
  - I had previously found crystallization methods for the following compounds:
    17β-estradiol • urea
    17α-estradiol • ½ H_2O
    17β-estradiol • ½ MeOH
    17β-estradiol • ⅔ MeOH • ⅓ H_2O

    The best conditions found to produce charge density quality crystals involve dissolving 17β-estradiol or 17α-estradiol in "wet" methanol. Allowing the solvent to evaporate as slowly as possible (~2-4 weeks) will yield charge density quality crystals. Unfortunately, this can result in the formation of different crystal systems (such as 17β-estradiol • ½ MeOH or 17β-estradiol • ⅔ MeOH • ⅓ H_2O). Selective crystallization was never achieved. This was probably due to the extremely small difference in packing energy of the different systems. "Wet" methanol is obtained by simply allowing methanol to sit for extended periods to absorb atmospheric water.
  - Some effort was made in the past year to obtain crystals of diethylstilbestrol (DES). This molecule was not listed in my statement of work, however it is a molecule known to interact strongly with the estrogen receptor an exhibit agonistic activity. It crystallizes in a centrosymmetric space group with the molecule sitting on a special position resulting in only half the molecule being unique. This makes it a good candidate for charge density studies. Unfortunately, slow evaporation studies and solvent diffusion studies using many solvents such as, isooctance, p-chlorophenol, acetonitrile, acetone, and several different types of alcohols were not successful. Only a powdery residue was observed.

- Temperature studies on each derivative to establish tolerances and the appropriate temperatures for the measurements.
  - Temperature studies were performed on the four crystal systems previously mentioned, as well as estrone and estriol. There were no problems observed with crystal stability in any of the systems when approaching liquid nitrogen temperatures. All of the systems were studied both in house and at the synchrotron source at Argonne National Labs in order to obtain data below liquid nitrogen temperatures (~20K) using liquid helium. We encountered problems with crystal stability when reaching such temperatures. Several attempts were made to cool the crystals by flash cooling as well as by cooling the crystals very slowly. Neither method improved the crystal stability at such low temperatures.

- Preliminary routine X-ray crystal structure determination on each derivative to check for composition, quality, and solvation.

  Preliminary data sets were collected on the four systems crystallized. Two of these structures were as expected. 17β-estradiol • ½ MeOH was a previously unknown structure and was electronically submitted to Acta Cryst.(1) The structure of the 17β-estradiol • ⅔ MeOH • ⅓ H_2O system was also new, however while chemically interesting, is not a good candidate for charge density research. The extreme number of atoms in the unit cell makes a detailed charge density study of the system very difficult. This system is, in fact very important chemically, because the three independent molecules in the asymmetric unit are not identical. While they share the same stereochemical configuration, they differ slightly in physical geometry. This structure is discussed in detail in the 1st publication from this study.(2) This publication is attached as supplemental material to this report.

Task 2. Electron density quality data collection on the above mentioned estrogen analogues.

- X-ray diffraction studies at liquid nitrogen temperatures on crystals that did not qualify for lower temperatures.
  - A complete data set of 17α-estradiol • ½ H_2O has been successfully collected and analyzed.
  - A complete data set of 17β-estradiol • urea has been successfully collected and analyzed.
  - A complete data set of 17β-estradiol • ½ MeOH been successfully collected and analyzed.

- X-ray diffraction studies at liquid helium temperatures.
  - Work has been continued to try to find a better strategy for cooling crystals down to near liquid He temperatures.

Task 3. Interpretation and analysis of nitrogen and helium temperature charge density data sets of above mentioned estrogen analogues.

- Analysis of the experimental data.
  - During this study it was discovered after attempting multipole refinements of the three systems that our process for data treatment was not consistent enough to yield reliable results. The problems lie in the integration of the raw data. This required that we take a step back and reevaluate the application of the software we use.
  - Integration of the raw data involves integrating the intensity of the reflections as measured by a two-dimensional CCD detector. Several parameters must be defined to determine exactly how the software integrates the reflections. It was the combination of parameters that had to be refined. There are three parameters which critically affect the outcome of the integration, and they are:
    - Box Size - area on 2-dimensional frame to be integrated for each reflection
    - Profile Fitting Limits – threshold for reflections which are used to determine the profiles applied in the fitting.
    - Simple Sum Perimeter Limit – Determines how far out on the reflection profile to integrate

    It was found that different detector settings, even for the same data set, require different box size parameters and profile fitting limits. The simple sum perimeter limit of 0.02 was found to be the best value for all three data sets. Selected crystal, integration, and reflection data for the three systems are shown in Appendix A.
  - Upon completion of the integration, more data treatment is required. This includes the absorption correction, data scaling, and statistical outlier determination.
  - The multipole model requires a local coordinate system be set up for every atom. A standard coordinate system was developed and applied to each structure where possible. The submitted version of the coordinate system paper is attached as supplemental material to this report.(3)
  - It was found that the starting values for the multipole model greatly influenced the path the refinement would take. It was determined that a specific set of starting values should be applied to each structure to ensure consistency. These optimum values are shown in Appendix A. .
  - The multipole refinement as well as full topological analysis was completed for all three structures.
    - 17β-estradiol • urea: As stated earlier in this study, the first data set was not usable. The second data set collected was of high quality. This allowed the multipole refinement to be completed.
    - 17β-estradiol • ½ MeOH: Despite the fact that the crystal system is P1, meaning there is no symmetry equivalent data which reduces redundancy in the data, the multipole refinement was successfully completed as well as full topological analysis.
    - 17α-estradiol • ½ H_2O: The water molecule of this system lies on a 2-fold axis of rotation, meaning only half of the molecule is unique. This in itself is not a problem except that it was discovered during the multipole refinement

that the hydrogen atom was very slightly disordered. The position it refined to generated a symmetry equivalent hydrogen atom which created an H – O – H bond angle of less than 90°. The thermal parameter of the hydrogen atom is twice as large as a typical hydrogen atom of the system. Due to the fact the disorder is a result of a shift on the order of 0.1 Angstroms for the hydrogen, the effect of this disorder is taken up by the large thermal parameter of the hydrogen. Unfortunately this disorder greatly effects the hydroxy atoms that are hydrogen bound to the water. This complicated the refinement significantly, however it was successfully completed as well as full topological analysis.

- The refinements were completed using κ and κ' parameters of 1.40 and 1.29 respectively. These values are critical because a hydrogen's isotropic thermal parameter is directly correlated to its κ and κ' parameters. These values were initially set at κ_{CH} = 1.40, 1.29 and κ_{OH} = 1.30, 1.29 because they gave the most appropriate ratio of thermal parameter magnitude, based on neutron data of other small organic molecules, between the hydrogen and the atom it is bound to. In the end the value of 1.20 was used for κ because it is a much more commonly accepted value. This required that a great deal of time be spent re-refining all three systems using the κ value of 1.20.

- Comparison of the results from the series of estrogen analogues.
  - Initial comparisons of the multipole models and the topological analysis have yielded expected and unexpected results. It was expected that the core structure of the estrogen molecules would remain relatively unchanged from system to system even with chemical substitutions at the activity-sensitive ends. This was found to be the case.
  - One major question that needed to be answered was could such small features as oxygen lone pair densities be determined on such large systems. If they could be determined, then you have to ask; Would they be affected by different hydrogen bonding schemes? Would the lone pair density of the oxygen's on the aromatic ring conjugate to the pi system of the aromatic ring? The answer is that we can determine features such as lone pair densities on the oxygen's (see diagrams in appendices). It was found that each oxygen atom had two lone pairs in a rough sp^3 type geometry. This demonstrates that the lone pairs are surprisingly robust in that they do not significantly change in different hydrogen bonding schemes and when the oxygen is bound to aromatic systems. This was somewhat surprising, however this type of analysis is not well represented in the literature.
  - Although the influence of the lattice is inherent in the multipole model of the estrogen molecule, the electrostatic potential is believed to provide a reasonable representation of a single molecule isolated from the crystal lattice. In these studies, the electrostatic potential of the hydroxy groups on the aromatic rings were consistent in both shape and magnitude. Generally covering nearly the entire lone pair region, the maximum magnitudes are ~-20 $eÅ^{-1}$. One could argue that this is expected given the consistency in the lone pair regions of the oxygen atoms. However, the C17 hydroxy groups are also consistent in their lone pair regions and they exhibit an interesting trend. The potential changes significantly

in both shape and magnitude based on the relative position of the hydroxy hydrogen with respect to H17. 17β-estradiol • urea and 17α-estradiol • ½ H_2O displayed a shift in the potential toward the lone pair region opposite H17, as well as increased magnitudes of ~ –35 and ~ –45 e$Å^{-1}$. H2O and H2O' were virtually opposite H17 in 17β-estradiol • ½ MeOH. This resulted in a fairly uniform distribution of the electrostatic potential with a maximum value of ~ –20 e$Å^{-1}$. Plots of the electrostatic potential are shown in Appendix A.

- The first paper in this series discusses the 17β-estradiol • urea system is completed and has been submitted for recommendation to The Proceedings of the National Academy of Sciences.
- The manuscript for the 17β-estradiol • ½ MeOH system is currently being prepared for submission to the Journal of the American Chemical Society.
- The manuscript for the 17α-estradiol • ½ H_2O system is currently being prepared for submission to the Journal of Physical Chemistry.

- Analyze relationship of charge density to receptor binding affinity and the chemical/biological effects as related to breast cancer.
  - Presumably there is a preferred orientation for the hydrogen of the C17 hydroxy group in the active site of the estrogen receptor. Unfortunately, the protein crystal structures determined to date do not have enough resolution to determine this. It seems possible that this is one mechanism by which the estrogen ligands could stimulate different responses from the estrogen receptor. Binding of different ligands would most likely result in different orientations of the C17 hydroxy hydrogen, thereby presenting different electrostatic potentials to the receptor. This could help to account for the changes in binding affinity and activity of the different estrogen derivatives.
  - Continued effort must be made to analyze more systems because a sample of three structures is not enough to confirm the trends that are appearing in the electron density and the electrostatic potential.

Key Research Accomplishments

- The core estrogen structure is very consistent between derivatives.
- Determination that it is possible to locate lone pair densities of oxygen's in such large systems
- Determination that the oxygen atoms of these systems are decidedly sp^3 in shape despite the fact they are bound to aromatic neighbors.
- Determination that the lone pairs appear to be unaffected by completely different hydrogen bonding environments.
- Determination that the electrostatic potential around the aromatic hydroxyl groups are consistent despite different hydrogen bonding environments.
- Determination that the electrostatic potential around the C17 hydroxy groups changes significantly in both shape and magnitude based on the relative position of the hydroxy hydrogen with respect to H17.

Reportable Outcomes

- Papers

1. Parrish, D.A. and A.A. Pinkerton, *Estradiol methanol hemisolvate.* Acta Crystallographica Section C, **1999**. 55(9): p. IUC9900100.
2. Parrish, D. A. and A.A. Pinkerton, *A New Structure of 1,3,5[10]-Estratriene-3,17β-diol Solvate: Estradiol 0.66(CH3OH)0.33(H2O).* Acta Crystallographica Section C, **2003**. C59: p. o80-o82.
3. Parrish, Damon A., A.A. Pinkerton, E.A. Zhurova, K. Poomani, and K. Kirschbaum, *A Standard Local Coordinate System for Multipole Refinements of the Estrogen Core Structure.* Journal of Applied Crystallography, (Submitted).
4. Parrish, Damon A., A.A. Pinkerton, E.A. Zhurova, *The Experimental Charge Density Study of Estrogens: 17β-Estradiol•Urea.* The Proceedings of the National Academy of Sciences, (Submitted for Recommendation).
5. Parrish, Damon A., A.A. Pinkerton, E.A. Zhurova, *The Experimental Charge Density Study of Estrogens: 17β-estradiol • ½ MeOH.* Journal of the American Chemical Society, (in preparation).
6. Parrish, Damon A., A.A. Pinkerton, E.A. Zhurova, *The Experimental Charge Density Study of Estrogens: 17α-estradiol • ½ H_2O.* Journal of Physical Chemistry, (in preparation).
7. Parrish, Damon A., Dissertation Title: Comparative Charge Density Studies of 17α-Estradiol and 17β-Estradiol

- Presentations

2000

i) American Crystallographic Association Meeting, St. Paul, MN, July 22-27.
   a) *Charge Density Distribution of Estrone.* Damon Parrish, Nan Wu, and A. Alan Pinkerton.

2002

i) DOD Breast Cancer Research Program Era of Hope Meeting, Orlando, FL, September 25-28.
   a) *Charge Density Studies of Three Estradiol Systems.* Damon A. Parrish and A. Alan Pinkerton.
   b) *Measurement of the Electron Density Distribution of Estrogens – a First Step to Advanced Drug Design.* A. Alan Pinkerton, Kristin Kirschbaum, Pumani Kumaradhas, Damon A. Parrish, Nan Wu and Elizabeth Zhurova

Conclusion

The ability to determine the electron density distribution of larger molecular systems such as estrogens has been clearly demonstrated. Observation of the consistency of the core structure of the estrogen molecule provides interesting chemical and physical information, as well as a basis for future estrogen studies. The robustness of the lone pairs under different hydrogen bonding conditions was unexpected. Finally, the trends in the electrostatic potential of the C17 hydroxy groups suggest a possible mechanism by which different estrogen ligands can elicit varied responses from the receptor. Proteins will react differently in their conformational changes to variations in the potential of the ligand. These actions/reactions will determine the downstream outcome of the protein complex. More studies of different estrogen derivatives, or the same derivatives with different orientations of the C17 hydroxy hydrogen, would help to support this hypothesis.

Career/Research Plans

As I stated in my original proposal, my career goals were to complete my PhD and to pursue a career in research crystallography, perhaps in the area of medicinal chemistry and rational drug design. Working on this project has given me the opportunity to do just that. I have received a three-year Postdoctoral Fellowship Award sponsored by the American Society for Engineering and Education (ASEE). This fellowship places me at the Naval Research Laboratory in Washington DC to provide crystallographic support for the National Institute on Drug Abuse (NIDA). I believe I was awarded this position based largely on my work with the estrogen systems. I would like to thank the DOD for their support of my work and for their facilitation in furthering my career. I would also like to say that I highly recommend Dr. Alan Pinkerton and his current graduate students as future candidates for this research award. Dr. Pinkerton and the University of Toledo provide an ideal environment for students to participate in an important area of research, which is in need of quality, knowledgeable people.

Appendix A

Crystal Data			
Chemical Formula	$C_{19}H_{28}N_2O_3$		
Temperature	100.0(1) K		
Crystal Dimensions	0.35 x 0.37 x 0.40 mm		
Space Group	$P2_12_12_1$		
a	7.9022(9) Å		
b	9.2228(10) Å		
c	24.5890(28) Å		
Volume	1792.06(56) $Å^3$		
Z (Crystallographic)	4		
Integration Parameters			
	Box Size (°)	Profile Fitting (I/σ)	Simple Sum Perimeter Limit
Low Angle	1.5 x 1.5 x 1.0	30/10	0.02
Medium Angle	1.2 x 1.2 x 0.8	30/10	0.02
High Angle	1.0 x 1.0 x 0.6	20/10	0.02
Reflection Statistics (from SORTAV)			
Total Reflections	110999		
Rejected Outliers	779		
Unique Reflections	13187		
Average Redundancy	8.4		
Resolution	1.180 $Å^{-1}$		
Completeness	98.6 %		
R_1	3.52 %		
R_2	3.98 %		
R_w	12.84 %		
Z (Refinement)	1.999		

Table A-1. Selected crystal, integration, and reflection data for 17β-estradiol • urea.

Crystal Data			
Chemical Formula	$C_{37}H_{52}O_5$		
Temperature	100.0(1) K		
Crystal Dimensions	0.22 x 0.26 x 0.42 mm		
Space Group	P1		
a	7.2934(1) Å		
b	9.2795(1) Å		
c	12.3918(2) Å		
α	89.4681(5)		
β	87.8569(4)		
γ	70.7659(4)		
Volume	791.290(33) $Å^3$		
Z (Crystallographic)	2		
Integration Parameters			
	Box Size (°)	Profile Fitting (I/σ)	Simple Sum Perimeter Limit
Low Angle	1.5 x 1.5 x 1.0	20/20	0.02
Medium Angle	1.2 x 1.2 x 0.8	20/20	0.02
High Angle	1.0 x 1.0 x 0.6	10/10	0.02
Reflection Statistics (from SORTAV)			
Total Reflections	86369		
Rejected Outliers	33		
Unique Reflections	29051		
Average Redundancy	3.0		
Resolution	1.329 $Å^{-1}$		
Completeness	91.9 %		
R_1	5.77 %		
R_2	5.34 %		
R_w	15.25 %		
Z (Refinement)	1.219		

Table A-2. Selected crystal, integration, and reflection data for 17β-estradiol • methanol.

Crystal Data			
Chemical Formula	$C_{18}H_{25}O_{2.5}$		
Temperature	100.0(1) K		
Crystal Dimensions	0.24 x 0.33 x 0.33 mm		
Space Group	C2		
a	19.0240(5) Å		
b	7.0652(2) Å		
c	13.3496(3) Å		
β	124.0553(10)		
Volume	1486.57(10) $Å^3$		
Z (Crystallographic)	4		
Integration Parameters			
	Box Size (°)	Profile Fitting (I/σ)	Simple Sum Perimeter Limit
Low Angle	1.2 x 1.2 x 0.8	40/10	0.02
High Angle	1.0 x 1.0 x 0.6	30/10	0.02
Reflection Statistics (from SORTAV)			
Total Reflections	85606		
Rejected Outliers	65		
Unique Reflections	14594		
Average Redundancy	5.9		
Resolution	1.319 $Å^{-1}$		
Completeness	98.2 %		
R_1	3.51 %		
R_2	3.88 %		
R_w	14.02 %		
Z (Refinement)	2.010		

Table A-3. Selected crystal, integration, and reflection data for 17α-estradiol • ½ H_2O.

	Charge	sp^2		sp^3
		20	33+	32-
O1	-0.50			
O2	-0.49			
C1	-0.30	-0.22	0.34	
C2	-0.38	-0.19	0.37	
C3	0.27	-0.21	0.38	
C4	-0.33	-0.17	0.36	
C5	-0.18	-0.22	0.33	
C6	-0.26			0.31
C7	-0.31			0.34
C8	-0.21			0.39
C9	-0.17			0.31
C10	-0.25	-0.18	0.37	
C11	-0.31			0.35
C12	-0.28			0.31
C13	-0.16			0.38
C14	-0.20			0.38
C15	-0.26			0.33
C16	-0.35			0.42
C17	0.20			0.38
C18	-0.32			0.27

	Charge
H1O	0.40
H2O	0.38
H1	0.23
H2	0.22
H4	0.26
H6x	0.20
H7x	0.17
H8	0.20
H9	0.16
H11x	0.17
H12x	0.16
H14	0.19
H15x	0.16
H16x	0.18
H17	0.13
H18x	0.18

Table A-4. Starting values entered into the model for the multipole refinements. Units for multipole populations are e^-.

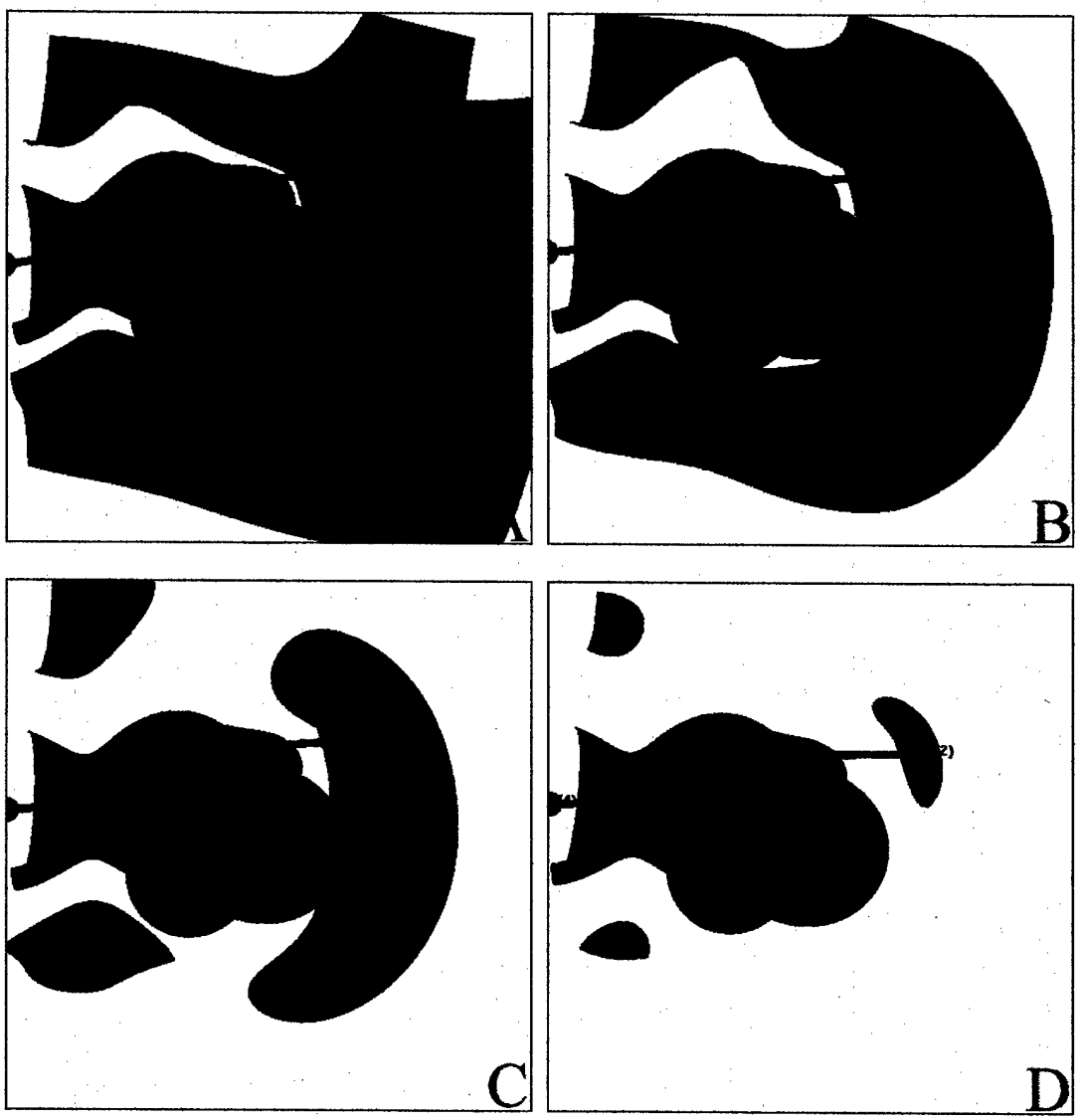

Figure A-1. Electrostatic potential isosurfaces of the O1 hydroxy group of 17β-estradiol • urea. The blue surface in each picture represents +1.0 eÅ^{-1}. The red surfaces represent the following potentials: A –0.05 eÅ^{-1}, B –0.10 eÅ^{-1}, C –0.15 eÅ^{-1}, D – 0.20 eÅ^{-1}.

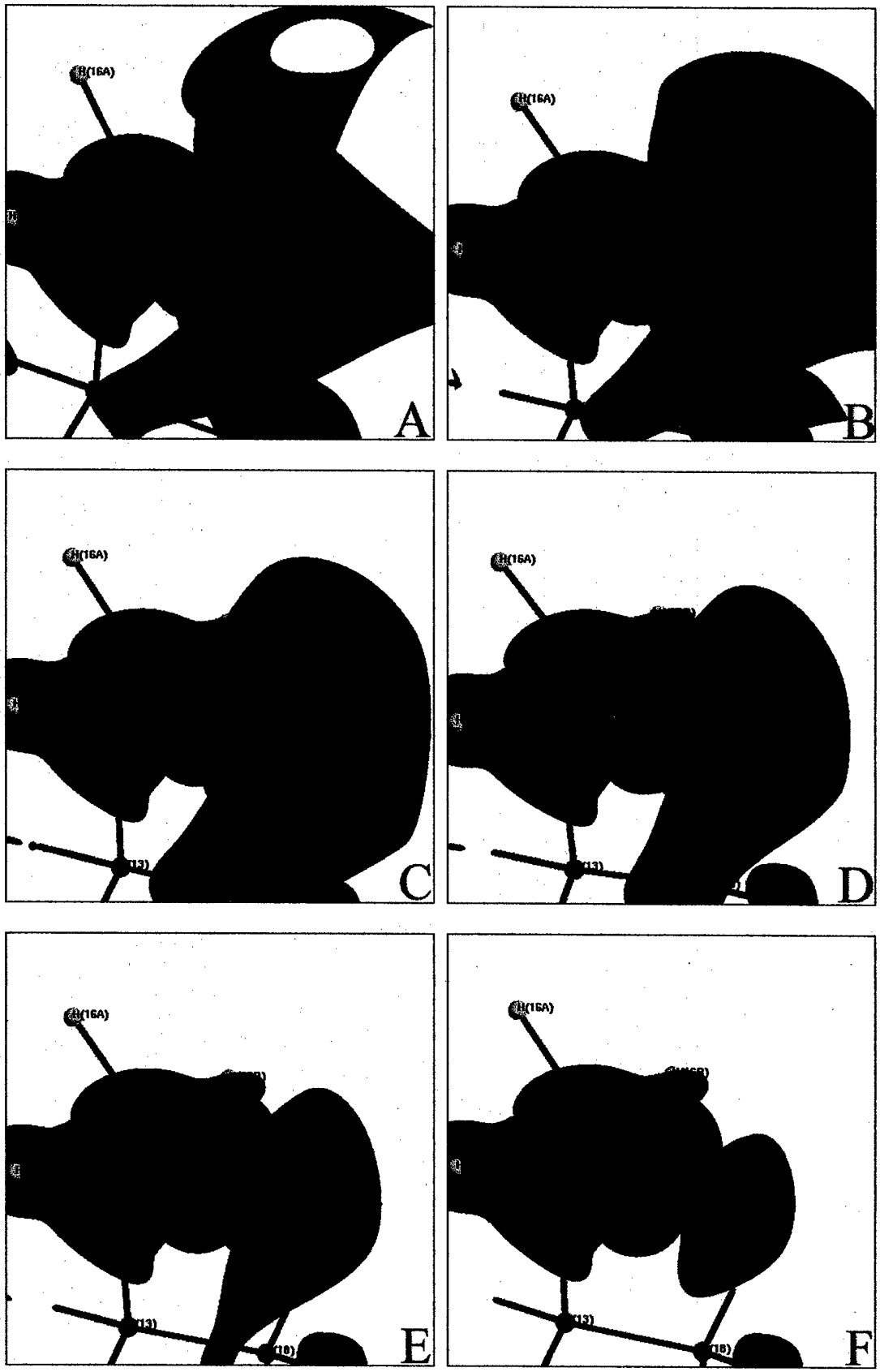
H(16A)
A
H(16A)
B
H(16A)
C
H(16A)
D
H(16A)
E
H(16A)
F

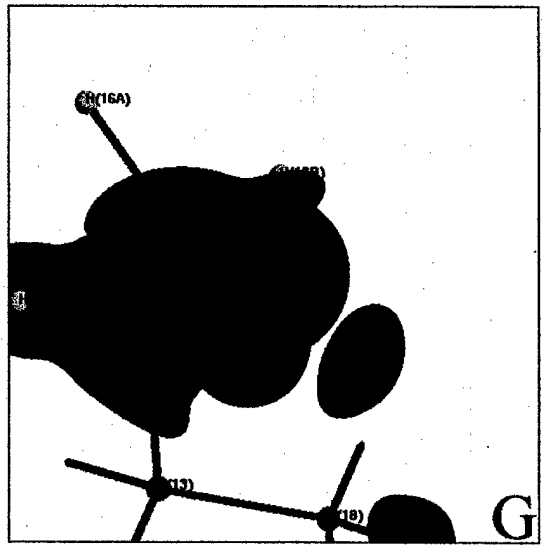

Figure A-2. Electrostatic potential isosurfaces of the O2 hydroxy group of 17β-estradiol • urea. The blue surface in each picture represents +1.0 eÅ^{-1}. The red surfaces represent the following potentials: A –0.05 eÅ^{-1}, B –0.10 eÅ^{-1}, C –0.15 eÅ^{-1}, D –0.20 eÅ^{-1}, E –0.25 eÅ^{-1}, F –0.30 eÅ^{-1}, G –0.35 eÅ^{-1}.

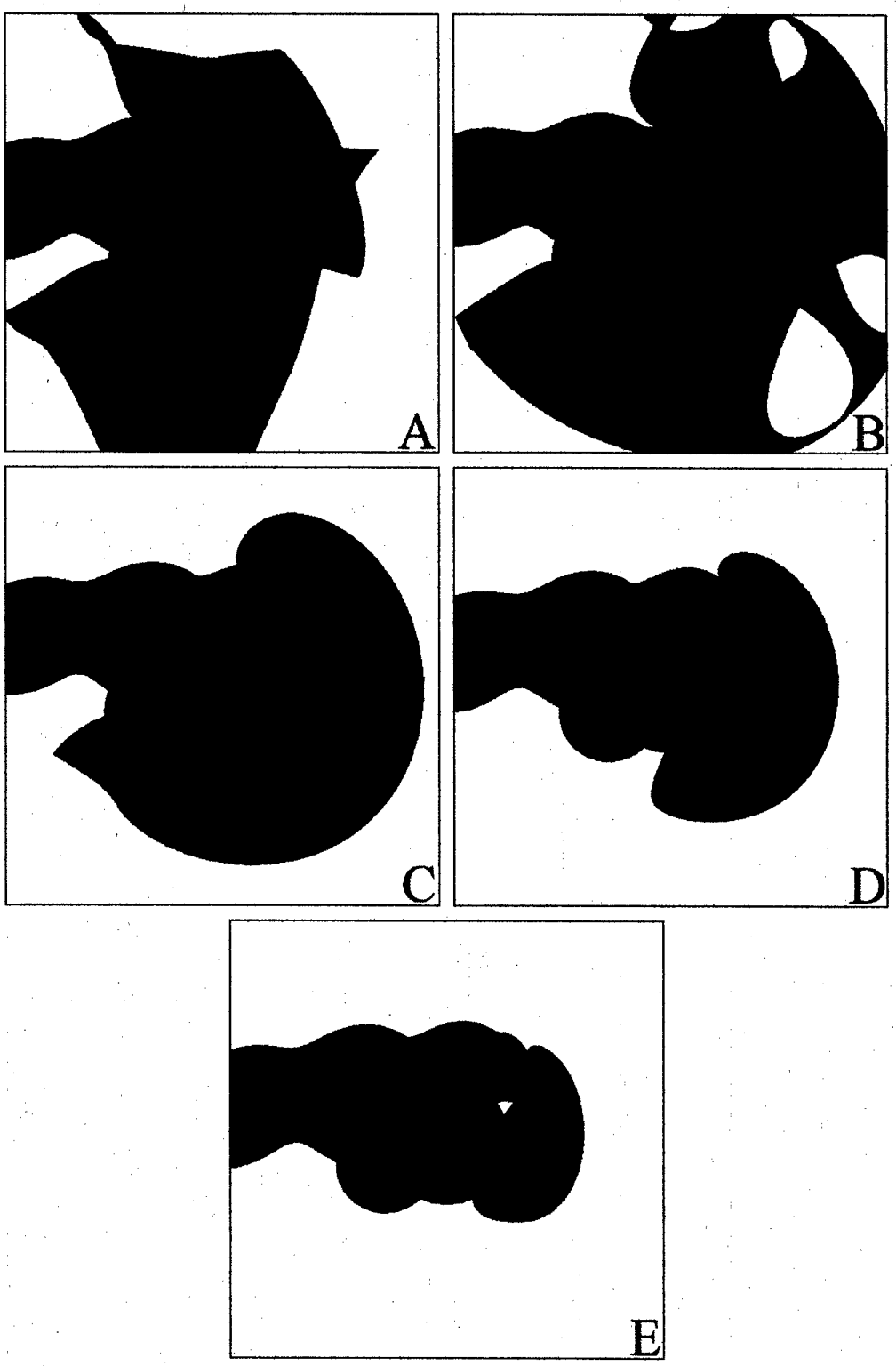

Figure A-3. Electrostatic potential isosurfaces of the O1 hydroxy group of 17β-estradiol • methanol. The blue surface in each picture represents +1.0 eÅ^{-1}. The red surfaces represent the following potentials: A –0.05 eÅ^{-1}, B –0.10 eÅ^{-1}, C –0.15 eÅ^{-1}, D – 0.20 eÅ^{-1}.

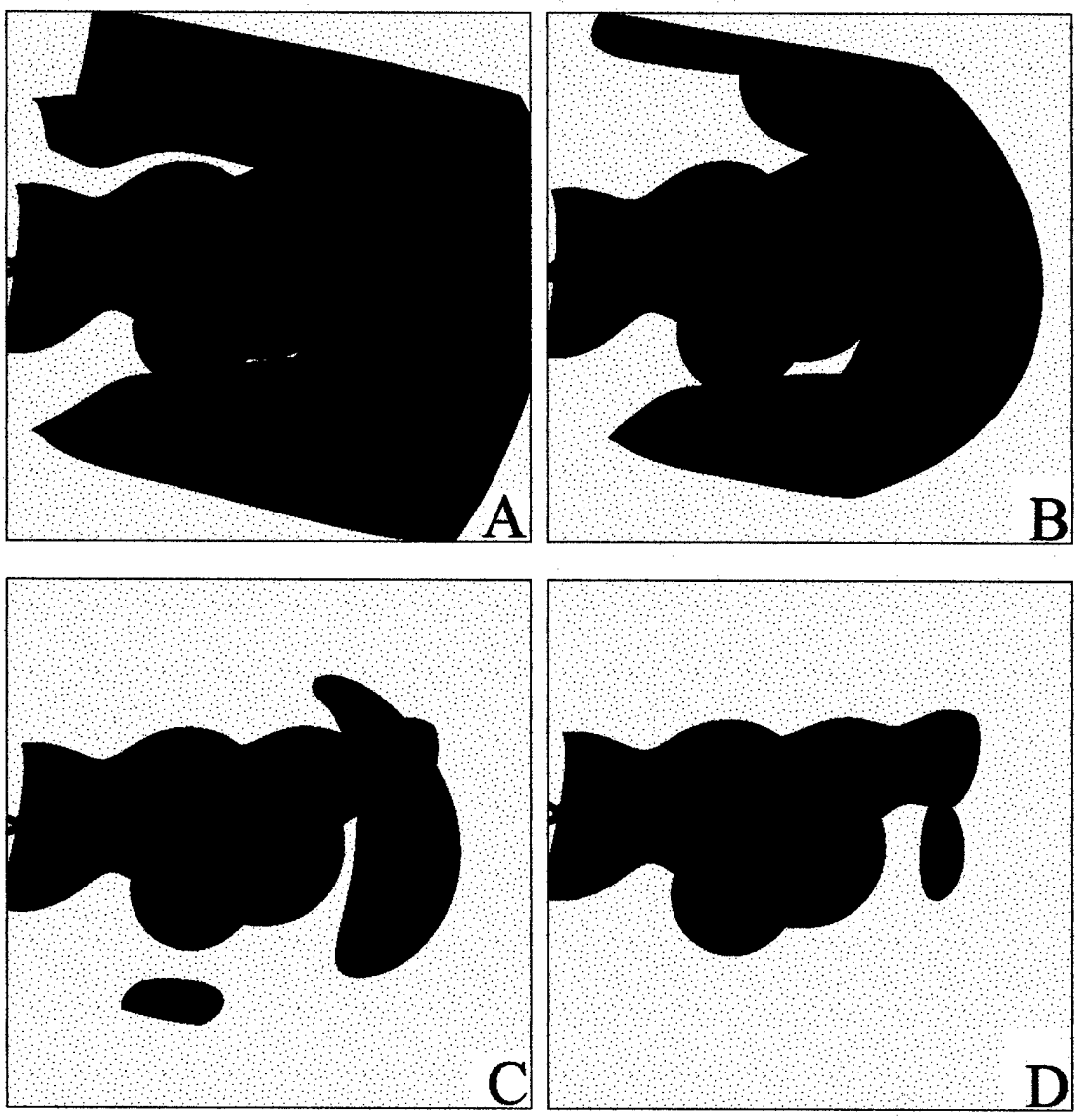

Figure A-4. Electrostatic potential isosurfaces of the O1' hydroxy group of 17β-estradiol • methanol. The blue surface in each picture represents +1.0 eÅ^{-1}. The red surfaces represent the following potentials: A –0.05 eÅ^{-1}, B –0.10 eÅ^{-1}, C –0.15 eÅ^{-1}, D – 0.20 eÅ^{-1}.

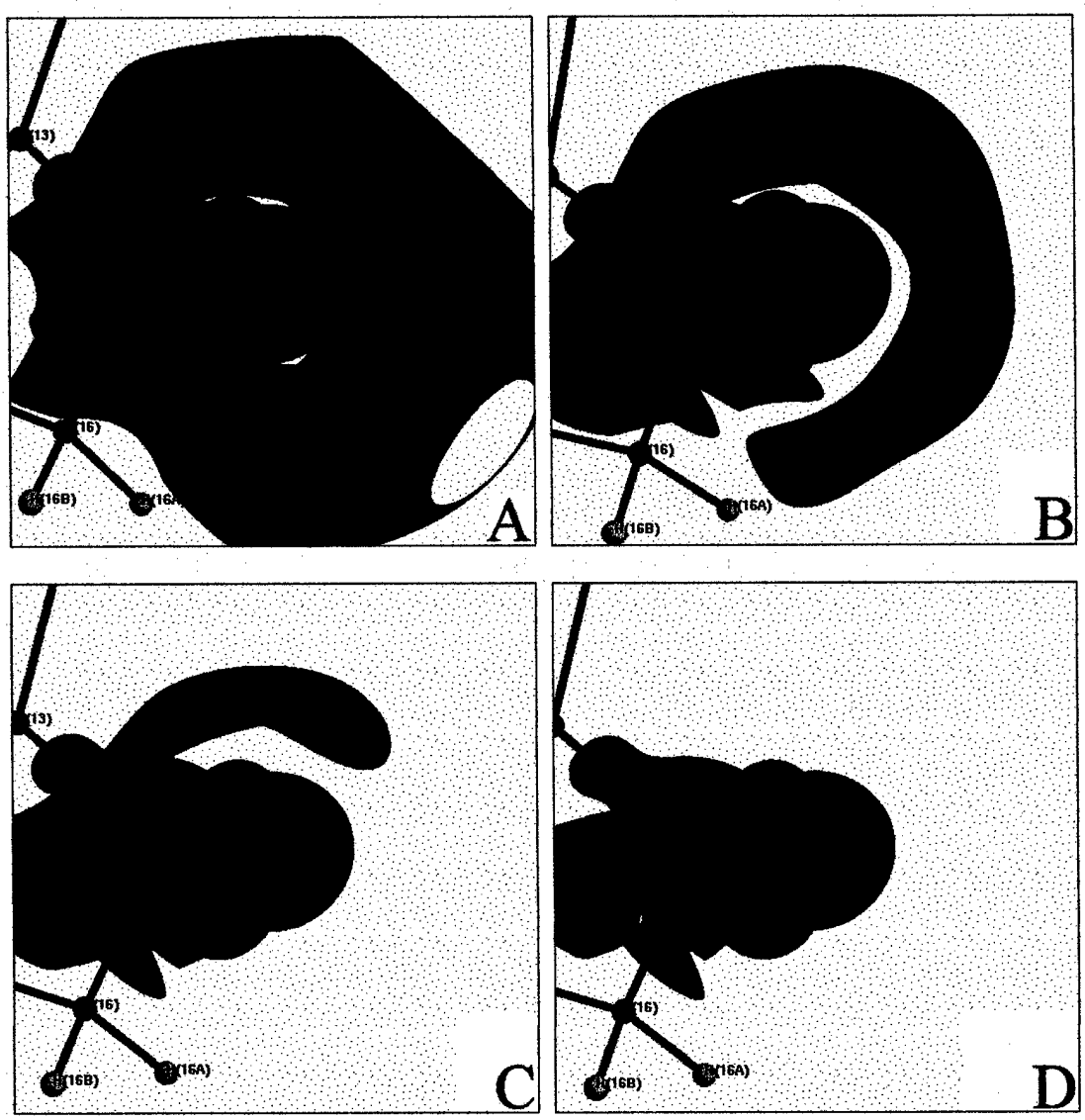

Figure A-5. Electrostatic potential isosurfaces of the O2 hydroxy group of 17β-estradiol • methanol. The blue surface in each picture represents +1.0 eÅ^{-1}. The red surfaces represent the following potentials: A –0.05 eÅ^{-1}, B –0.10 eÅ^{-1}, C –0.15 eÅ^{-1}, D – 0.20 eÅ^{-1}.

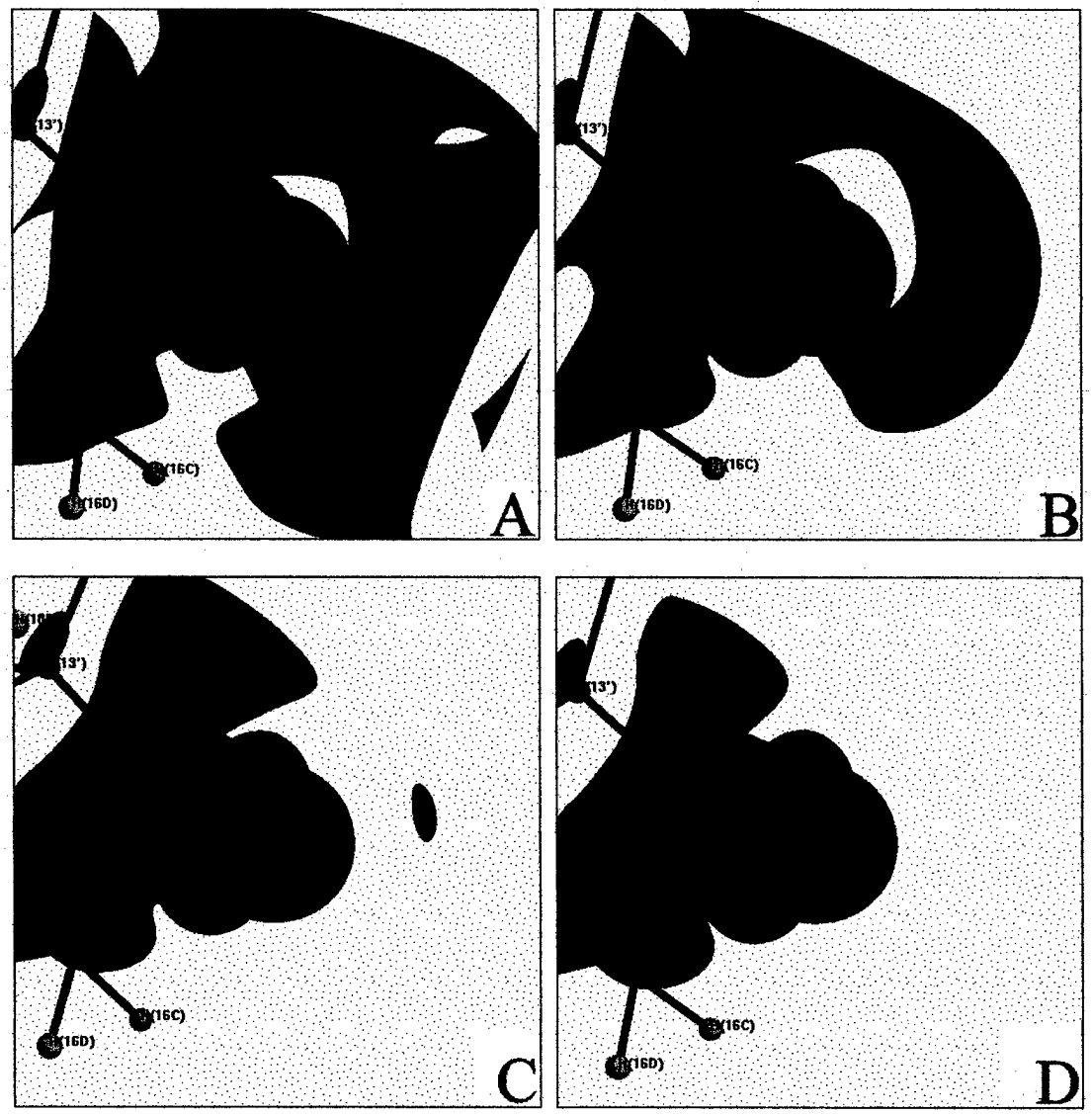

Figure A-6. Electrostatic potential isosurfaces of the O2' hydroxy group of 17β-estradiol • methanol. The blue surface in each picture represents +1.0 eÅ^{-1}. The red surfaces represent the following potentials: A –0.05 eÅ^{-1}, B –0.10 eÅ^{-1}, C –0.15 eÅ^{-1}, D – 0.20 eÅ^{-1}.

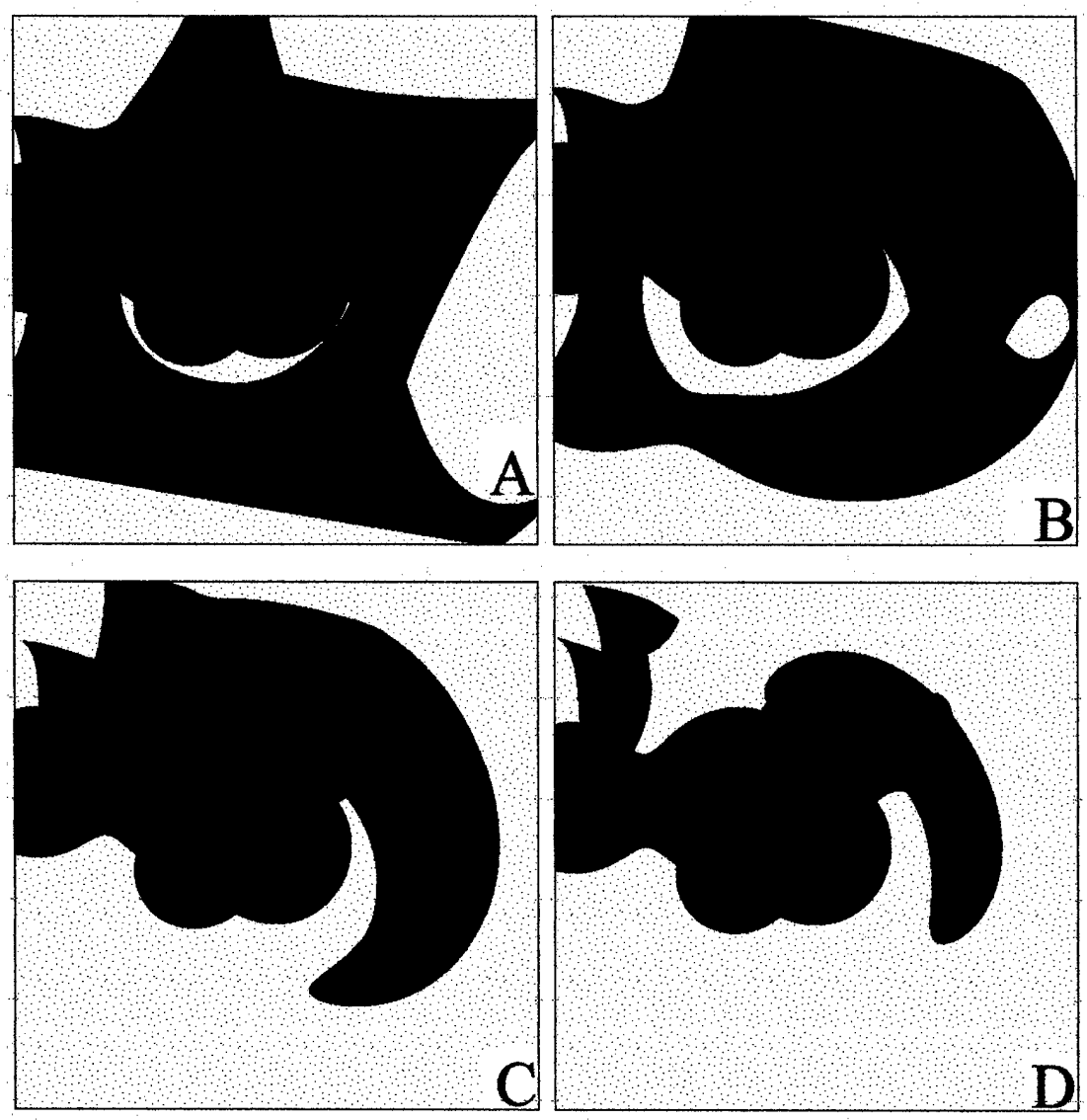

Figure A-7. Electrostatic potential isosurfaces of the O1 hydroxy group of 17α-estradiol • ½ H_2O. The blue surface in each picture represents +1.0 eÅ^{-1}. The red surfaces represent the following potentials: A –0.05 eÅ^{-1}, B –0.10 eÅ^{-1}, C –0.15 eÅ^{-1}, D – 0.20 eÅ^{-1}.

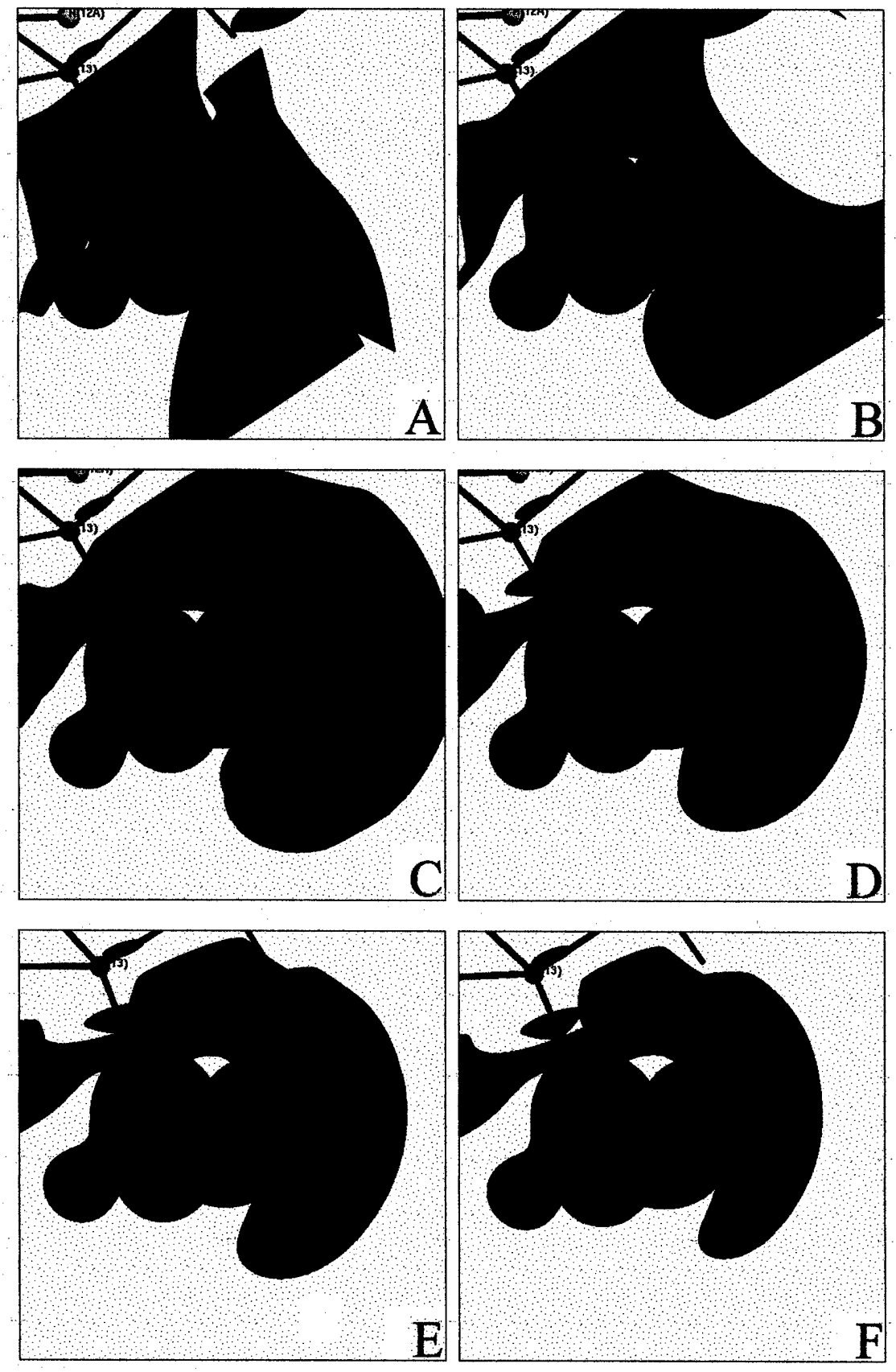
A
B
C
D
E
F

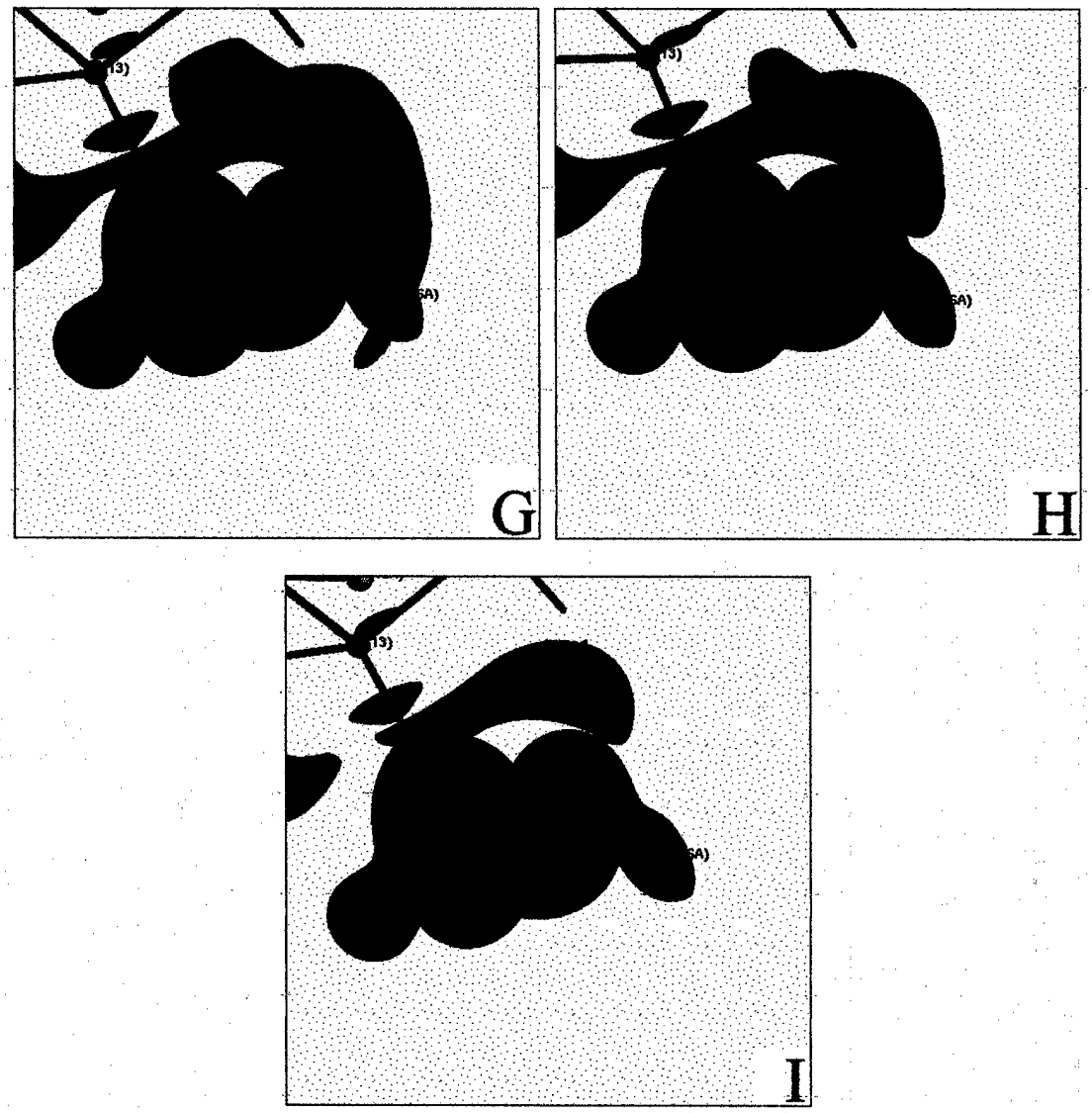

Figure A-8. Electrostatic potential isosurfaces of the O2 hydroxy group of 17α-estradiol • ½ H_2O. The blue surface in each picture represents +1.0 eÅ^{-1}. The red surfaces represent the following potentials: A –0.05 eÅ^{-1}, B –0.10 eÅ^{-1}, C –0.15 eÅ^{-1}, D –0.20 eÅ^{-1}, E –0.25 eÅ^{-1}, F –0.30 eÅ^{-1}, G –0.35 eÅ^{-1}, H –0.40 eÅ^{-1}, I –0.45 eÅ^{-1}.

Current information:

Dr. Damon Parrish
Research Chemist
Naval Research Laboratory, Code 6030
4555 Overlook Ave.
Washington, DC 20375
Phone: (202)404-2141
Fax: (202)767-6874
Email: dparrish@ccs.nrl.navy.mil

Acta Crystallographica Section C
Crystal Structure Communications
ISSN 0108-2701

A new estra-1,3,5(10)-triene-3,17β-diol solvate: estradiol–methanol–water (3/2/1)

Damon A. Parrish and A. Alan Pinkerton*

Department of Chemistry, University of Toledo, Toledo, Ohio 43606, USA
Correspondence e-mail: apinker@uoft02.utoledo.edu

Received 22 October 2002
Accepted 21 November 2002
Online 25 January 2003

The title solvate of the steroid 17β-estradiol (E_2) with methanol and water, $C_{18}H_{24}O_2 \cdot 0.67CH_4O \cdot 0.33H_2O$, is the first E_2 derivative to contain three crystallographically independent molecules in the asymmetric unit. The three steroid molecules, along with two methanol molecules and a water molecule, create a three-dimensional hydrogen-bonded system. Three-sided columns are formed, with the estradiol molecules aligned lengthwise parallel to (101), and joined by solvent molecules at both hydrophilic ends. The three estradiol molecules differ slightly in their ring-bowing angles, *i.e.* the angle between the mean plane of the *A* ring and that of the *BCD* ring; this angle ranges from 7.1 to 12.2°.

Comment

17β-Estradiol, E_2, is a member of the estrogen family of hormones. In recent years, interest in these molecules has focused primarily on understanding their biological role in initiating breast cancer. It is well known that their ability to form hydrogen bonds in the active site of the estrogen receptor (ER) influences biological activity. This ability to form hydrogen bonds has been clearly demonstrated in an array of crystal structures, especially in that of E_2, containing different solvent molecules or other hydrogen-bond acceptors.

When comparing these structures, the flexibility of the hydrophobic region of the molecule, more specifically the *B* ring, becomes very apparent. Several papers have already discussed the ring bowing of this molecule (Cooper *et al.*, 1969; Cody *et al.*, 1971; Busetta *et al.*, 1976; Duax *et al.*, 1979). Weise & Brooks (1994) took it a step further, performing molecular-modeling calculations on observed and novel confirmations. Ivanov and co-workers carried out a related study which included a larger body of compounds and more detailed analysis (Ivanov *et al.*, 1998). They concluded that there are two possible conformations very close in energy, which differ in the *B*-ring arrangement, although the chance of the strained-geometry binding is low, as one quarter of the binding energy (−11.9 kcal mol^{-1}; 1 kcal mol^{-1} = 4.184 kJ mol^{-1}) is predicted to be lost (Anstead *et al.*, 1997). The point initially postulated by Weise & Brooks remains, *i.e.* that the flexibility to allow bending or other conformational changes of the ligand in the receptor appears energetically achievable, and this could be an important property in determining their activity.

Molecular-dynamics studies on the ligand-binding domain (LBD) of the ER demonstrate that the motion of the LBD requires the *A* ring to remain fairly steady while the *CD* ring retains a higher degree of freedom. The range of motion found in that study (Maalouf *et al.*, 1998) agrees very well with the reported crystal structures. It is well known that the hydrogen bonding of the ligand in the LBD causes conformational changes in the receptor. This seemingly accommodating motion of the LBD and the ligand supports the idea postulated by Weise & Brooks that the flexibility of E_2, or of any other ligand which enters the LBD, could also effect the activity of the ligand. A more rigid or flexible ligand could change the natural motion of the ER complex, resulting in a change in activation factor (AF-2) activity, and therefore possibly effecting co-activator recruitment. This process is not well understood; the flexibility of the ligand is certainly only one of many physical factors associated in the activity of E_2. The structure of the title solvate, (I), continues the trend in observing the flexibility of this molecule from a structural and hydrogen-bonding point of view, while the molecule lies in the lowest energy conformation.

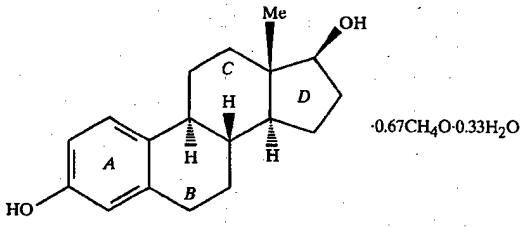

(I)

The crystal of (I) contains three crystallographically unique E_2 molecules (Fig. 1). The *B* rings of the E_2 molecules adopt the typical conformation of a distorted 7α,8β-half-chair, and this is responsible for most of the structural flexibility. Calculation of the ring-bowing angle, as defined by Duax & Norton (1975), reveals a range of 5.1° for the three molecules. Table 1 compares the ring-bowing angles of the currently

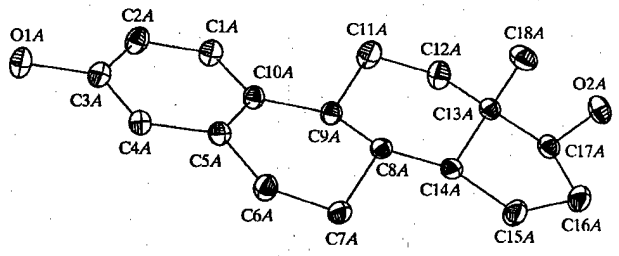

Figure 1
A view of molecule *A* of (I), with the atom-numbering scheme; the other two molecules are similarly labeled, with the corresponding suffix *B* or *C*. Displacement ellipsoids are plotted at the 50% probability level. The solvent molecules have been omitted for clarity.

  DOI: 10.1107/S0108270102021637

known E_2 crystal structures. The spread of over 12°, with angles found distributed over the entire range, indicate the shallowness of the potential associated with the bowing deformation. In a system as dynamic as the human body, the molecule would certainly have a wide range of conformations easily available.

The packing of (I) results in three-sided cylinders of estradiol molecules arranged parallel to (101), with the C18 methyl group pointing towards the center (Fig. 2). This, of course, aligns the large hydrophobic regions of the molecules, as well as the hydrophilic hydroxy groups. These cylinders then stack on top of each other, creating three-sided columns (Fig. 3) held together by hydrogen bonds involving the hydroxy groups and the three solvent molecules. A more detailed picture of the hydrogen bonding between the solvent and E_2 molecules can be seen in Fig. 4 and from the data in Table 3. There is also an intercolumnar hydrogen bond, which occurs between the water molecule and a 3-hydroxy group. This, along with the intercolumnar hydrogen-bonded solvent,

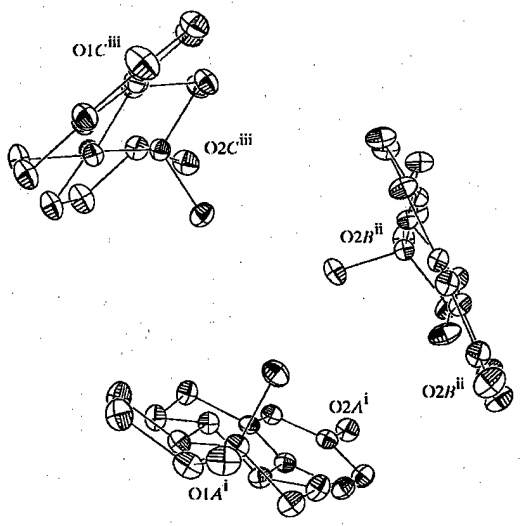

Figure 2
The molecular arrangement of (I), looking down the three-sided column. Displacement ellipsoids are plotted at the 50% probability level [symmetry codes: (i) x, y, z; (ii) $-2-x, y-\frac{1}{2}, -1-z$; (iii) $x-1, y, z$].

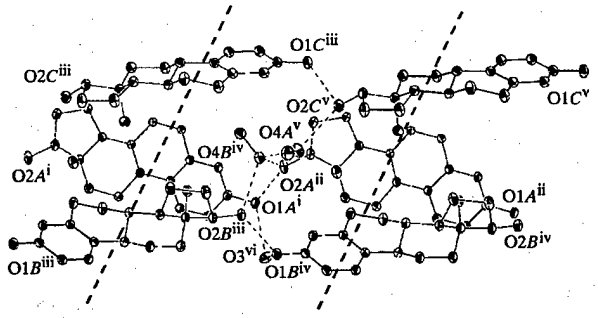

Figure 3
The packing of E_2 groups in (I), with the hydrogen-bonded solvent molecules, viewed perpendicular to the columns. Dotted lines indicate the region detailed in Fig. 4. Displacement ellipsoids are plotted at the 50% probability level [symmetry codes: (i) x, y, z; (ii) $1+x, y, 1+z$; (iii) $-2-x, y-\frac{1}{2}, -1-z$; (iv) $-1-x, y-\frac{1}{2}, -z$; (v) $x, y, 1+z$; (vi) $-x, y-\frac{1}{2}, -z$].

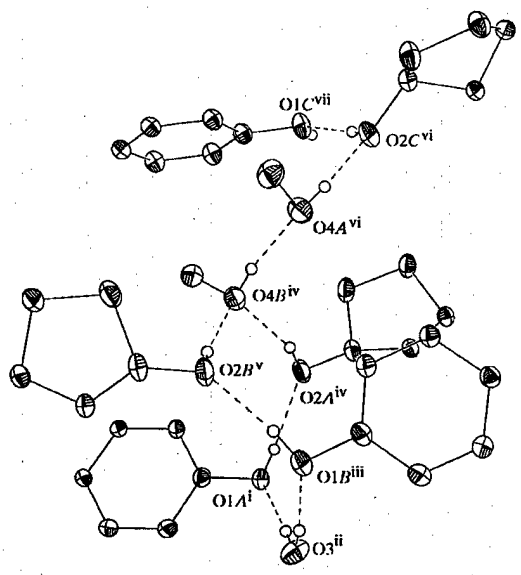

Figure 4
The hydrogen-bonded region of the column shown in Fig. 3, including the solvent molecules and only the *A* or *D* rings of E_2. Displacement ellipsoids are plotted at the 50% probability level [symmetry codes: (i) x, y, z; (ii) $-x, y-\frac{1}{2}, -z$; (iii) $-1-x, y-\frac{1}{2}, -z$; (iv) $1+x, y, 1+z$; (v) $-2-x, y-\frac{1}{2}, -1-z$; (vi) $x, y, 1+z$; (vii) $-1-x, y, z$].

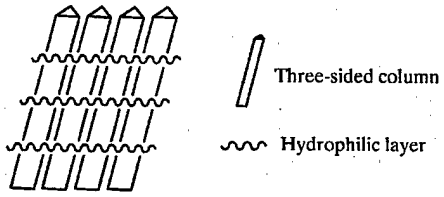

Figure 5
A schematic diagram of the packed columns in (I) and their relation to the hydrophilic layer containing the hydroxy groups and solvent molecules.

creates a hydrophilic layer which is approximately 30° from the perpendicular to the columns (Fig. 5). Structurally, all bond lengths and angles are in expected ranges (Table 2).

Experimental

Crystals were grown by slow evaporation from a methanol solution open to the air. It is presumed that the methanol was either wet prior to use in this experiment or absorbed atmospheric moisture. Crystals of (I) were grown over the course of 3 d and harvested when reaching the appropriate size.

Crystal data

$C_{18}H_{24}O_2 \cdot 0.67CH_4O \cdot 0.33H_2O$
$M_r = 299.74$
Monoclinic, $P2_1$
$a = 11.7152$ (4) Å
$b = 19.6270$ (6) Å
$c = 12.1310$ (4) Å
$\beta = 117.978$ (1)°
$V = 2463.34$ (14) Å^3
$Z = 6$
$D_x = 1.212$ Mg m^{-3}
Ag $K\alpha$ radiation
Cell parameters from 7309 reflections
$\theta = 2.3$–27.9°
$\mu = 0.05$ mm^{-1}
$T = 298$ (1) K
Cuboid, colorless
0.4 × 0.3 × 0.3 mm

Data collection

Siemens SMART Platform CCD area-detector diffractometer
ω scans
Absorption correction: empirical *via* multipole expansion (Blessing, 1995) using *SADABS* (Sheldrick, 1996)
T_{min} = 0.840, T_{max} = 0.985
44 195 measured reflections
21 122 independent reflections
15 597 reflections with $I > 2\sigma(I)$
R_{int} = 0.048
θ_{max} = 27.9°
$h = -18 \rightarrow 19$
$k = -32 \rightarrow 29$
$l = -20 \rightarrow 20$

Refinement

Refinement on F^2
$R[F^2 > 2\sigma(F^2)]$ = 0.058
$wR(F^2)$ = 0.145
S = 0.99
21 122 reflections
698 parameters
H atoms treated by a mixture of independent and constrained refinement
$w = 1/[\sigma^2(F_o^2) + (0.0812P)^2]$ where $P = (F_o^2 + 2F_c^2)/3$
$(\Delta/\sigma)_{max}$ = 0.001
$\Delta\rho_{max}$ = 0.41 e Å^{-3}
$\Delta\rho_{min}$ = −0.23 e Å^{-3}

Table 1
Comparison of ring-bowing angles (°) in reported E_2 crystal structres.

Compound	Molecule 1 angle	Molecule 2 angle	Molecule 3 angle
17β-estradiol–0.5H_2O†	15.6		
17β-estradiol–propanol†	12.9		
17β-estradiol–urea†	5.6		
17β-estradiol–0.5MeOH‡	10.4	3.4	
(I)§	12.2	11.9	7.1

† Wiese & Brooks (1994). ‡ Parrish & Pinkerton (1999). § This work.

Table 2
Selected bond lengths (Å).

O1*A*—C3*A*	1.3716 (18)	O2*A*—C17*A*	1.4354 (19)
O1*B*—C3*B*	1.3792 (17)	O2*B*—C17*B*	1.4305 (19)
O1*C*—C3*C*	1.3691 (18)	O2*C*—C17*C*	1.4400 (19)

Table 3
Hydrogen-bonding geometry (Å, °).

D—H···*A*	*D*—H	H···*A*	*D*···*A*	*D*—H···*A*
O1*A*—H1O*A*···O2*A*^{i}	0.74 (3)	1.89 (3)	2.6226 (17)	171 (3)
O1*B*—H1O*B*···O2*B*^{i}	0.85 (3)	1.83 (3)	2.6654 (18)	171 (3)
O1*C*—H1O*C*···O3	0.76 (3)	1.82 (3)	2.5767 (18)	170 (3)
O2*A*—H2O*A*···O4*B*	0.76 (3)	1.97 (3)	2.7017 (18)	162 (2)
O2*B*—H2O*B*···O4*B*^{ii}	0.73 (2)	2.06 (2)	2.7823 (19)	168 (2)
O2*C*—H2O*C*···O1*C*^{iii}	0.73 (2)	1.99 (3)	2.7169 (17)	175 (3)
O3—H3O*A*···O1*A*^{iv}	0.72 (4)	2.02 (4)	2.743 (2)	178 (4)
O3—H3O*B*···O1*B*^{v}	0.76 (3)	2.04 (3)	2.7926 (19)	173 (3)
O4*A*—H4O*A*···O2*C*	0.83 (3)	1.85 (3)	2.6809 (18)	174 (3)
O4*B*—H4O*B*···O4*A*^{vi}	0.78 (2)	1.88 (2)	2.6462 (17)	166 (2)

Symmetry codes: (i) $1+x, y, 1+z$; (ii) $-3-x, \frac{1}{2}+y, -2-z$; (iii) $x-1, y, z-1$; (iv) $-x, \frac{1}{2}+y, -z$; (v) $1+x, y, z$; (vi) $x-1, y, z$.

The absolute configuration of the E_2 molecules in (I) was known from the natural product starting material. The intensity data were corrected for decay and absorption using *SADABS* (Sheldrick, 1996). All H atoms of the solvent molecules and the hydroxy groups of the E_2 molecules were located in a difference map and refined with isotropic displacement parameters. The remaining H atoms were included with idealized geometries (C—H = 0.96–0.98 Å), and their isotropic displacement parameters were refined.

Data collection: *SMART* (Bruker, 1998); cell refinement: *SAINT* (Bruker, 1999); data reduction: *SAINT*; program(s) used to solve structure: *SHELXS*97 (Sheldrick, 1990); program(s) used to refine structure: *SHELXL*97 (Sheldrick, 1997); molecular graphics: *SHELXTL* (Siemens, 1994); software used to prepare material for publication: *SHELXTL*.

We thank the College of Arts and Sciences of the University of Toledo for generous financial support of the X-ray diffraction facility.

Supplementary data for this paper are available from the IUCr electronic archives (Reference: SQ1003). Services for accessing these data are described at the back of the journal.

References

Anstead, G. M., Carlson, K. E. & Katzenellenbogen, J. A. (1997). *Steroids*, **62**, 268–303.
Blessing, R. H. (1995). *Acta Cryst.* A**51**, 33–58.
Bruker (1998). *SMART*. Version 5.622. Bruker AXS Inc., Madison, Wisconsin, USA.
Bruker (1999). *SAINT*. Version 6.20. Bruker AXS Inc., Madison, Wisconsin, USA.
Busetta, B., Barrans, Y., Precigoux, G. & Hospital, M. (1976). *Acta Cryst.* B**32**, 1290–1292.
Cody, V., DeJarnette, F., Duax, W. & Norton, D. A. (1971). *Acta Cryst.* B**27**, 2458–2468.
Cooper, A., Norton, D. A. & Hauptman, H. (1969). *Acta Cryst.* B**25**, 814–828.
Duax, W. L. & Norton, D. A. (1975). In *Atlas of Steroid Structures*. New York: Plenum.
Duax, W. L., Rohrer, D. C., Blessing, R. H., Strong, P. D. & Segaloff, A. (1979). *Acta Cryst.* B**35**, 2656–2664.
Ivanov, J., Mekenyan, O., Bradbury, S. P. & Schuurmann, G. (1998). *Quant. Struct. Activity Rel.* **17**, 437–449.
Maalouf, G. J., Xu, W. R., Smith, T. F. & Mohr, S. C. (1998). *J. Biomol. Struct. Dyn.* **15**, 841–852.
Parrish, D. A. & Pinkerton, A. A. (1999). *Acta Cryst.* C**55**, IUC9900100.
Sheldrick, G. M. (1990). *Acta Cryst.* A**46**, 467–473.
Sheldrick, G. M. (1996). *SADABS*. University of Göttingen, Germany.
Sheldrick, G. M. (1997). *SHELXL*97. University of Göttingen, Germany.
Siemens (1994). *SHELXTL*. Release 5.03. Siemens Analytical X-ray Instruments Inc., Madison, Wisconsin, USA.
Wiese, T. E. & Brooks, S. C. (1994). *J. Steroid Biochem. Mol. Biol.* **50**, 61–73.

A Standard Local Coordinate System for Multipole Refinements of the Estrogen Core Structure

Yu-Sheng Chen, Kristin Kirschbaum, Poomani Kumaradhas, Damon A. Parrish, A. Alan Pinkerton,* and Elizabeth A. Zhurova

Department of Chemistry, University of Toledo, 2801 W. Bancroft Street, Toledo, OH 43606, USA. E-mail: apinker@uoft02.utoledo.edu

Synopsis The initiation of a comparative charge density study on a series of estrogen derivatives revealed the need for a standardized local coordinate system for each atom in order to facilitate comparison of the multipole refinements. Herein we propose such a system for the core structure of a generic estrogen molecule and suggest starting parameters for the population of the most prominent multipoles.

Abstract A comparative charge density study on a series of estrogen derivatives has been initiated. The study utilizes the Hansen-Coppens atom centered multipole model to describe the valence electron density distribution. Direct comparison of the population parameters for each estrogen after the respective multipole refinements requires standardization of the atom centered local coordinate systems. Such a standard coordinate system for the common estrogen core is reported, taking advantage of the shape of those multipoles which have the spatial characteristics of sp^2 and sp^3 hybrid orbitals. Additionally, populating these principal multipoles at the beginning stage of the refinements improves the stability of these large, highly correlated calculations.

Keywords: Estrogen; charge density; coordinate system

1. Introduction

Recent advances in computers, software, and X-ray data collection technology have made charge density studies on a series of larger "small molecules" in a reasonable amount of time feasible. A comparative charge density analysis has been initiated to study a series of estrogen derivatives.

Electron density refinements from experimental X-ray diffraction data have been performed using the XD suite of programs (Koritsanszky et al., 1995), which utilizes the Hansen-Coppens model to describe the valence electron density (Coppens 1997, Hansen & Coppens 1978). This model is based on multipole expansions centred on the atoms and

concomitantly requires a user defined local Cartesian coordinate system for each atom in the structure .

In a comparative study, consistency in this model setup is essential to enable direct comparison of the parameters of the multipole refinements for different molecules in a related series. This article proposes a standard local coordinate system for the atoms of the core structure of a generic estrogen molecule.

As well as being responsible for the development of secondary sexual characteristics, it has been determined that some estrogens are responsible for the initiation and progression of certain types of breast cancer. This study attempts characterization of the physical and electronic features of these molecules and the relationship of such submolecular properties to biological activity.

Most biologically active estrogens are A-ring or D-ring isomers of the naturally occuring estradiol or derivatives thereof, containing the same hydrocarbon ring core structure. With careful choice of directions, the local coordinate system can take advantage of the spatial characteristics of certain multipoles that, if populated, would mimic the shape of the bonding electron density derived from sp^2 and sp^3 hybrid orbitals.[1] (Pichon-Pesme et al., 1995; Coppens, 1997) This allows a majority of the valence electron density to be modelled by the linear combination of only a few multipoles. Given the number of parameters for such large, non-centrosymmetric systems, typically greater than 40 atoms, this approach can considerably stabilize the initial multipole refinements. By using a standard coordinate system, upon completion of the multipole refinement, a rational comparison can then be made among various related charge density studies.

The 17β-estradiol molecule, along with the labelling scheme of the core structure, is shown in scheme 1. For all methylene groups, hydrogen atoms on the same side of the core as the methyl group at position 18 are labelled b, those on the other side are labelled a. The C and D rings projected down the C18-C13 bond are provided as an insert to define the orientation of the methyl group hydrogen atoms.

[1] It is important to distinguish between the multipoles, which are density functions, and orbitals, which are derived from wavefunctions.

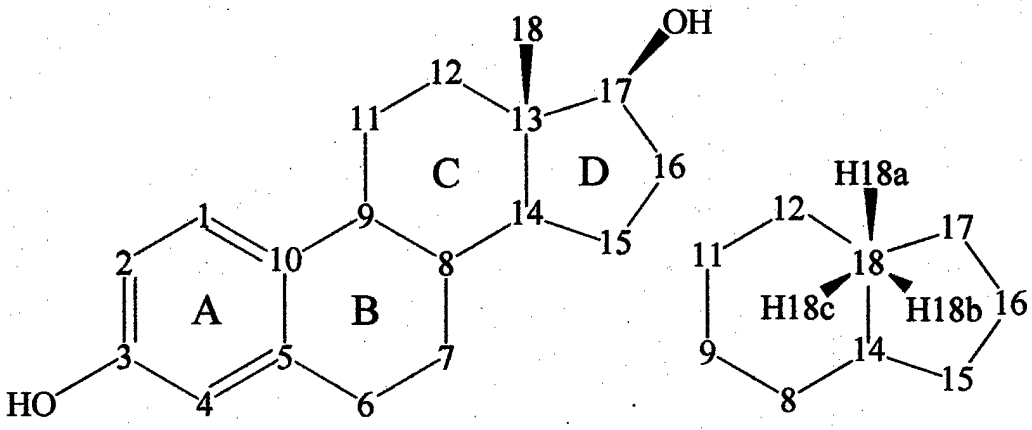

Scheme 1

2. Method

The cartesian axes *x,y,z* of the above mentioned atom centered coordinate systems are calculated in the program XD (Koritsanszky et al., 1995) based on two user defined vectors. In general, the first vector ($\mathbf{v}_1$) for a given atom (1) originates at its nucleus, is directed towards another atom (2) in the system - or, if necessary, a "dummy" atom - and defines axis(1). A second vector ($\mathbf{v}_2$) with the same origin points towards another atom (3), or dummy atom, describing the axis(1) - axis(2) plane. A third vector ($\mathbf{v}_3$) is taken perpendicular to this plane,

$$\mathbf{v}_1 = (\mathbf{r}_2 - \mathbf{r}_1) \qquad \mathbf{v}_2 = (\mathbf{r}_3 - \mathbf{r}_1) \qquad \mathbf{v}_3 = \mathbf{v}_1 \times \mathbf{v}_2$$

where $\mathbf{r}_1$, $\mathbf{r}_2$, and $\mathbf{r}_3$ are the position vectors of atom(1), atom(2), and atom(3), respectively. An orthonormal vector triplet ($\mathbf{e}_{ax1}$, $\mathbf{e}_{ax2}$, $\mathbf{e}_{ax3}$) is then formed which we have chosen to be right handed.

$$\mathbf{e}_{ax1} = \mathbf{v}_1/|\mathbf{v}_1| \qquad \mathbf{e}_{ax2} = (\mathbf{v}_3 \times \mathbf{v}_1)/|(\mathbf{v}_3 \times \mathbf{v}_1)| \qquad \mathbf{e}_{ax3} = \mathbf{v}_3/|\mathbf{v}_3|$$

Although axes 1, 2 and 3 can be assigned labels *x,y,z* arbitrarily, for the current molecules we define axis(1) as *x*, axis(2) as *y*, and axis(3) as *z* for non-hydrogen atoms, and axis(1) as *z*, axis(2) as *y* and axis(3) as *x* for hydrogen atoms.

Given these assignments, the valence electron density of the aromatic sp^2 type carbons atoms in the A-ring (scheme 1), can be initially approximated by populating two multipoles, the 33+ and 20. Pictorial representations of the angular function for these multipoles can be seen in Figure 1. Defining the *xy* plane of the coordinate system to lie in the plane of the bound atoms, i.e. the aromatic plane, will allow the positive lobe of the 33+ octupole to align with the three covalent bond regions. The 20 quadrupole will then be positioned perpendicular to this plane, a negative populations adding to the in plane σ bonding and depopulating the p orbital as required for π bond formation.

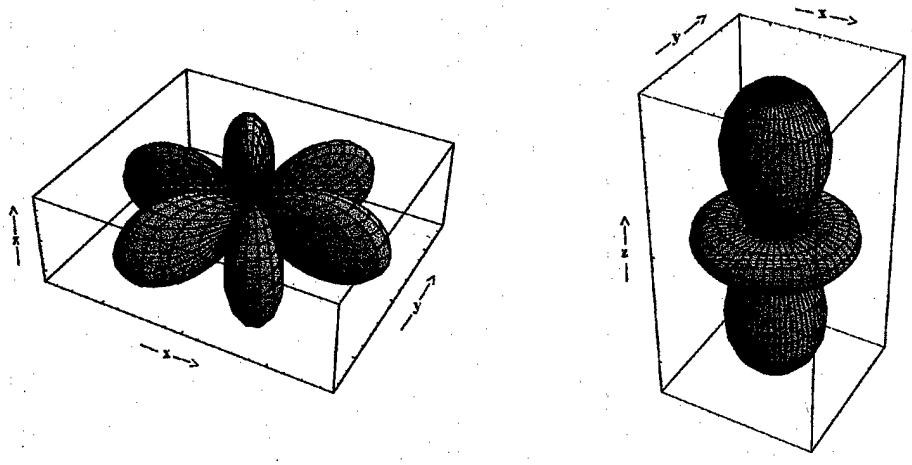

Figure 1 Coordinate system and angular functions of the 33+ and 20 multipoles with blue representing positive regions and red, negative. Functions visualized using MATLAB (2000).

The covalent bonding regions of the sp^3 type carbon atoms in the B, C, and D-rings of the generic estrogen can effectively be modelled by a single multipole, the 32- octupole. The axes associated with the 32- octupole do not correspond to the populated regions, hence two "dummy" atoms must be used to define the local coordinate system in this case. Their positions are calculated on the bisectors of the bond angles (the two-folds axes of the tetrahedron) at the atom of interest. An example of an sp^3 coordinate system and the 32-octupole is shown in Figure 2.

Approximation of the bond density of the hydrogen atoms can be achieved by initially populating a single dipole along *z*. A complete list of vector definitions for carbon and hydrogen atoms for the estrogen core are given in Tables 1 and 2. Using this standardized set of coordinates systems for future theoretical and experimental electron density studies on estrogen derivatives (and possibly expanding it for other steroids like progesterone) it will be possible to compare individual multipole populations for different molecules in this series.

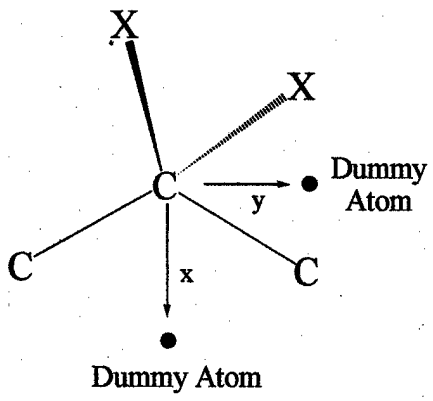

X = C or H

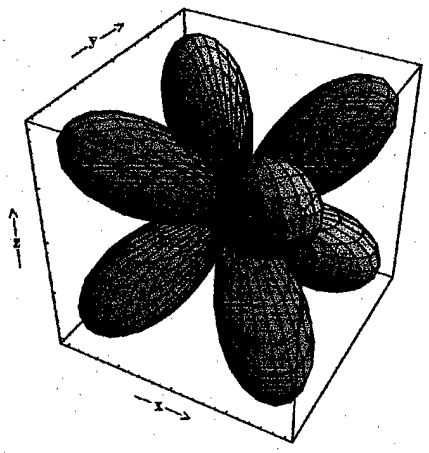

Figure 2 Model coordinate system for a sp^3 type atom and 32- multipole, with blue representing positive density and red, negative. (MATLAB, 2000).

Populating these principal multipoles at the beginning stage of the refinements may improve the stability of these large, highly correlated calculations. We have thus listed suitable values for the core structure based on our own refinements (Chen et al., 2003) of six different estrogen molecules (Table 3). We note that the sum of the monopole populations do not sum to zero for the estrogen core. To maintain electroneutrality, it is essential that appropriate starting values be assigned to other substituents, e.g. for estradiol, values of –0.47 and 0.29 would be appropriate monopole populations for the O and H atoms of the hydroxy groups.

3. Conclusion

Examples of typical input for the XD program and pictorial representation of the coordinate schemes for the hydrocarbon core of estrogens as recommended in this paper are available as supplementary material.

Table 1 Atoms used to define vectors $\mathbf{v}_1$ and $\mathbf{v}_2$ for carbon atoms[a]

Atom(1)	Atom (2)	Atom(3)
C1	C2	C10
C2	C3	C1
C3	C4	C2
C4	C5	C3
C5	C10	C4
C6	Dum1 (C5 - C7)	Dum2 (C5 - H6a)
C7	Dum3 (C6 - C8)	Dum4 (C6 - H7a)
C8	Dum5 (C7 - C9)	Dum6 (C7 - C14)
C9	Dum7 (C8 - C11)	Dum8 (C8 - C10)
C10	C1	C5
C11	Dum9 (C9 - C12)	Dum10 (C12 - H11a)
C12	Dum11 (C11 - C13)	Dum12 (C13 - H12a)
C13	Dum13 (C12 - C14)	Dum14 (C14 - C17)
C14	Dum15 (C8 - C15)	Dum16 (C8 - C13)
C15	Dum17 (C14 - C16)	Dum18 (C14 - H15a)
C16	Dum19 (C15 - C17)	Dum20 (C15 - H16a)
C17	Dum21 (C13 - C16)	Dum22 (C16 - O2)
C18	Dum23 (H18a - H18b)	Dum24 (H18b - H18c)

[a] Bond lengths of atoms used to calculate dummy atom positions (in parentheses) are adjusted to be equidistant from the atom of interest to ensure a true bisection.

Table 2. Atoms used to define vectors $\mathbf{v}_1$ and $\mathbf{v}_2$ for hydrogen atoms

Atom(1)	Atom(2)	Atom(3)
H1	C1	C9
H2	C2	H1
H4	C4	O1
H6a	C6	H6b
H6b	C6	H6a
H7a	C7	H7b
H7b	C7	H7a
H8	C8	C13
H9	C9	H14
H11a	C11	H11b
H11b	C11	H11a
H12a	C12	H12b
H12b	C12	H12a
H14	C14	H9
H15a	C15	H15b
H15b	C15	H15a
H16a	C16	H16b
H16b	C16	H16a
H17	C17	O2
H18a	C18	H18b
H18b	C18	H18c
H18c	C18	H18a

Table 3: Initial set of population parameters for the most important multipoles.

		sp^2		sp^3			
Atom	00	20	33+	32-	Atom	00	10
C1	-0.22(3)	-0.22(5)	0.32(5)		H1	0.24(4)	0.14(4)
C2	-0.28(7)	-0.21(5)	0.34(5)		H2	0.24(4)	0.15(4)
C3	0.15(4)	-0.18(5)	0.34(7)		H4	0.23(4)	0.16(2)
C4	-0.26(5)	-0.20(4)	0.33(4)		H6x	0.18(4)	0.15(2)
C5	-0.13(3)	-0.22(4)	0.36(7)		H7x	0.18(4)	0.14(2)
C6	-0.27(4)			0.31(7)	H8	0.19(4)	0.13(5)
C7	-0.28(6)			0.31(6)	H9	0.18(2)	0.12(4)
C8	-0.18(6)			0.38(5)	H11x	0.18(4)	0.12(2)
C9	-0.16(6)			0.33(9)	H12x	0.18(4)	0.14(4)
C10	-0.13(3)	-0.20(3)	0.36(4)		H14	0.18(3)	0.14(3)
C11	-0.28(6)			0.33(4)	H15x	0.19(5)	0.12(4)
C12	-0.28(5)			0.32(6)	H16x	0.17(5)	0.15(3)
C13	-0.21(6)			0.38(7)	H17	0.10(2)	0.18(2)
C14	-0.15(4)			0.34(3)	H18x	0.14(3)	0.13(4)
C15	-0.32(7)			0.30(7)			
C16	-0.35(5)			0.32(7)			
C17	0.16(4)			0.30(5)			
C18	-0.39(6)			0.22(6)			

Hydrogen labels such as H6x, represent both H6A and H6B. Populations are average values from 6 studies on - 17β-estradiol.½MeOH, 17β-estradiol.urea, 17α-estradiol, 17α-estradiol.½H_2O, 16α,17β - estriol, estrone. κ's for H atoms were fixed at 1.4. Other values for κ would be expected to introduce small changes to the refined monopole populations, but to have minimal effect on the higher poles.

Acknowledgements We thank to the Department of Defense, USAMRMC for financial support (Grants DAMD17-00-1-0468 and DAMD17-99-1-9408)

References

Chen Yu-S., Kirschbaum K., Kumaradhas P., Parrish D.A., Pinkerton A.A., Wu N., Zhurova, E.A. (2003) to be published.

Coppens P. (1997) *X-Ray Charge Density Analysis and Chemical Bonding* (Oxford University Press, Oxford)

Hansen, N.K. and Coppens P. (1978) *Acta Cryst.* A34, 909-921.

Koritsanszky T., Howard S., Mallison P.R., Su Z., Richter T., and Hansen N.K. (1995) XD. A Computer Program Package for Multipole Refinement and Analysis of Electron Densities from Diffraction Data. Free University of Berlin, Berlin.

MATLAB Version 6. (2000) The Mathworks Inc., Natick, MA USA.

Pichon-Pesme V, Lecomte C., and Lachekar H. (1995) *J. Phys. Chem.* 99, 6242-6250.

Physical Sciences: Chemistry

The Experimental Charge Density Study of Estrogens: 17β-Estradiol•Urea
(135 Character limit)

Damon Parrish and A. Alan Pinkerton
Chemistry Department, University of Toledo, 2801 West Bancroft Street, Toledo, Ohio 43606

Corresponding Author:

Dr. A. Alan Pinkerton
Chemistry Department
University of Toledo
2801 West Bancroft Street
Toledo, Ohio 43606
Phone: 419-530-4580
Fax: 419-530-4033
Email: apinker@uoft02.utoledo.edu

Manuscript Information:

Number of Text Pages: (6 pg limit)

Number of Figures:

Number of Tables:

Abstract word count: (250 word limit)

Character count: (47000 Character limit)

In order to relate molecular electrostatic potential to biological activities of estrogens, a comparative charge density study of different derivatives has been initiated. The first completed charge density analysis of this series for 17β-estradiol•urea is presented here. It has been demonstrated that it is possible to perform a quality experimental charge density study for the big organic system with 56 atoms in the non-centrosymmetric space group. The special tools such as the optimal coordinate system and slow initially constrained refinement have been used to accomplish this study.

Our results for the urea molecule reasonably agree with the previous experimental and theoretical results showing the quality of our data. In the 17β-estradiol molecule, oxygen atoms appeared to be sp^3 in shape, exhibiting two consistent, distinct lone pairs despite of different chemical environments. No interaction of hydroxy group oxygen lone pairs with the π orbitals of the aromatic ring has been observed. The analysis of the electrostatic potential revealed that the negative potential in the lone pair region of the oxygen atoms is quite different. The Bader's topological analysis has been performed, and atomic charges have been estimated. The results are compared and discussed.

Estrogens are known to be responsible for the development of secondary sexual characteristics, as well as they effect growth, differentiation and function of wide range of tissues [1]. It has also been shown [2] that some estrogens are responsible for the initiation and progression of certain types of breast cancer. These molecules have the ability to bind as ligands to the estrogen receptor in the first of many steps which could result in the activation (agonistic effect) or repression (antagonistic effect) of genes critical in the mechanism of tumor growth. While the mechanism by which the estrogens influence cancer is currently unknown, subtle changes in the chemical structure of estradiol and the other estrogens are known to elicit different biological responses in the development of cancer. It has been suggested [3] that the agonistic/antagonistic responses of the different estrogens can be related to such physical properties as their electrostatic potential and charge density distribution.

A comparative charge density study of a series of estrogen derivatives has been initiated in our group, with the primary goal of relating the electronic and physical structure of the molecule to biological action. In addition to molecular properties, charge density studies provide significant

fundamental information about the functional groups and the atoms which make them up, helping to investigate basic chemical principles of small organic molecules in general. This paper will pay particular attention to the hydroxy groups of the estrogen molecule. The hydroxy groups are some of the most chemically interesting portion of the estrogen molecule, and their interaction with the receptor is thought to be mostly responsible for their activity.

Described here is the charge density study of 17β-estradiol•urea. This particular crystal system was chosen to be the first in the series for two reasons. First, 17β-estradiol (E_2) is the most common naturally occurring estrogen and is typically the standard by which all other estrogenic activities are related. E_2 demonstrates an agonistic response in *in vitro* tests which typically utilize the estrogen receptor in either competitive yeast or human cell assays [4-5]. Secondly, it contained a solvated urea molecule which has been extensively studied. Both theoretical and experimental charge density studies have been performed on this molecule [6-7]. This provides a direct means of comparison to test our methods against previous results.

Experimental

Data Collection and Reduction

Crystals were grown by slow evaporation as described by Duax in the original publication of the crystal structure [8]. The clear, colorless crystal of approximate dimensions 0.35 × 0.37 × 0.40 mm was attached to a 30 μm carbon fiber using a small amount of epoxy resin. Data were collected at 100.0(1) K on a Bruker Platform Diffractometer equipped with a SMART 6000 CCD area detector located at 7.12 cm from the goniometer center. The Oxford Cryostream system has been used to cool the crystal. The crystals were irradiated with graphite monochromated Mo K_α radiation (λ = 0.7107 Å). 0.3° omega scans were carried out at four phi settings and three detector positions in 2θ, resulting in more than 7400 frames. A frame time of 60 seconds was used for the low angle setting, and 180 seconds for the medium and high angle settings. A complete experimental protocol is deposited.

The intensities were integrated using the program *SAINT* [9]. After several integrations and preliminary refinements, it was found that different integration parameters were required for each detector setting to obtain the best possible structure factors. The box sizes, profile fitting parameters, and the simple sum perimeter limits were adjusted for each detector setting. The unit cell parameters have been finally refined in *SAINT* using a total of 9999 reflections.

Lorentz-polarization and $\lambda/2$ corrections were applied to the integrated intensities with a $\lambda/2$ correction factor of 0.0012, this value being taken from the earlier study [10]. The program

SORTAV [11] was used for outlier determination, averaging, and applying the absorption correction. Only reflections with $I > 3\sigma(I)$ and below 1.00 $Å^{-1}$ were used during the multipole refinements.

Table 1. The crystal information and experimental details.

Formula	$C_{19}H_{28}N_2O_3$
Formula Weight	332.43
Crystal System	Orthorhombic
Space Group	$P2_12_12_1$
a	7.9022(9) Å
b	9.2228(10) Å
c	24.5890(28) Å
$\alpha = \beta = \gamma$	90.0°
Volume	1792.06 $Å^3$
Z	4
T	100.0 K
λ	0.7107 Å
$(\sin \theta/\lambda)_{max}$	1.180 $Å^{-1}$
Reflections Collected	110999
Rejected Outliers	779
Unique Reflections	13187
Included in the Refinement [$I > 3\sigma(I)$]	7626
Data completeness	98.6 %
Average redundancy	8.4
R_{int}	0.0411
R_1 (spherical)	0.065
wR_2 (spherical)	0.145
$R(F^2)$ [$I > 3\sigma(I)$] (multipole)	0.029
$R(F^2)$ all data (multipole)	0.036
wR (F^2)	0.045
Weighting scheme	$1/\sigma^2$
Goodness of Fit	1.393

Least-Squares Refinements

The crystal structure was re-solved, and the spherical atom model was refined using the program *SHELXL-97* [12]. 17β-estradiol and urea molecules are shown in Figure 1. All hydrogen atoms were located from the difference Fourier map. The results of this refinement served as the starting point for the aspherical atom refinements that were performed using the *XD* software package [13].

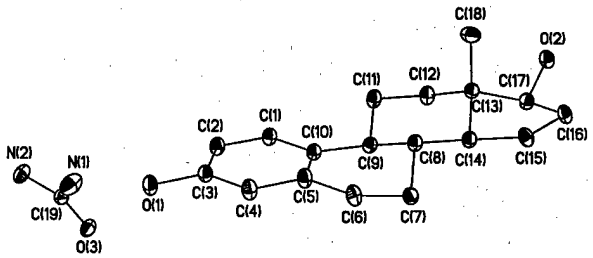

Figure 1. 17β-estradiol and urea molecules showing 50% probability thermal ellipsoids as at 100K. Hydrogen atoms are omitted for clarity.

The aspherical atom model [14], used in further refinements consists of three components. The first and second describe spherically averaged core and valence densities normalized to one electron, while the third one describes the aspherical valence density. $\rho(\mathbf{r})$ is the electron density, P_c, P_v, and P_{lm} are population coefficients, the core population (P_c) was fixed in this study. Asphericity is taken into account by expanding of the electron density over real combinations of spherical harmonics, y_{lm}, which satisfy local symmetry. The variable radial parameters, κ and κ', allow for expansion or contraction of the valence terms. R_l are normalized Slater-type radial functions.

$$\rho_{atomic}(\mathbf{r}) = P_c\rho_{core} + P_v\kappa^3\rho_{valence}(\kappa r)$$

$$+ \sum_{l=1}^{4} \kappa'^3 R_l(\kappa' r) \sum_{m=-l}^{l} P_{lm} y_{lm}(\mathbf{r}/r)$$

Because the model is based on atom centered multipoles, a coordinate system is required for each atom in the system. The core structure of the estrogen molecule was set up using the standard estrogen coordinate system to take advantage of the shape of certain multipoles to increase the stability of the initial multipole refinements [15]. The vectors for the oxygen atoms of the estrogen molecule were directed to bound atoms. The coordinate system setup for the urea molecule is deposited.

Before the refinements were begun, the hydrogen atom positions were corrected by extending the X – H distances to their neutron bond lengths ($C_{sp2}H$ = 1.08 Å, $C_{sp3}H$ = 1.10 Å, $C_{sp3}H_2$ = 1.09 Å, $C_{sp3}H_3$ = 1.06 Å, OH = 0.97 Å, $N_{sp2}H_2$ = 1.01 Å). These values were fixed in the refinement. A well known correlation exists between the thermal parameter and the kappa parameters of a hydrogen atom, only allowing the kappa parameters to be refined when the thermal parameters of the hydrogen atom are known [16]. To avoid this problem, fixed kappa values (κ_H = 1.20 and κ'_H = 1.20) were used, while the thermal parameters were allowed to refine [17-18].

Initially, to reduce the number of parameters in the least squares process, chemical constraints and only the most significant multipoles were considered. By the end of the refinement, all non-hydrogen atoms were treated up to the octupole level with no chemical constraints. The hydrogen atoms were refined with only two multipoles having cylindrical symmetry along the X - H bond. Hydrogen atoms bound to the same carbon have been constrained to be equal. The electroneutrality constraint has been imposed on both of two molecules. Complete tables giving the final structural information, such as atomic coordinates, U_{ij}'s, U_{iso}'s, bond lengths, bond angles and multipole parameters are deposited.

Topological Analysis, Atomic Charges and Electrostatic Potential

The topological analysis was performed based on the Atoms in Molecules (AIM) Quantum Theory [19]. The *XD* property assessment program, *XDPROP*, was used to perform a quantitative critical point* analysis on all covalent and hydrogen bonding interactions, as well as oxygen lone pair densities. The atomic basin boundaries were defined and the atomic charges (Bader's charges) were integrated within the basins with the program *TOPXD* [20]. The integrated atomic charge $q(\Omega)$ over the atomic basin Ω is defined as a difference between nuclear Z_Ω and electronic $N(\Omega)$ charges:

* Critical points are special points in the electron density, where $\nabla\rho(\mathbf{r}_{CP})=0$. The saddle (3,-1) point reflects the chemical bonding. In the Laplacian, the (3,+3) minimum point corresponds to the maximum curvature of the electron density in the charge concentration regions. See ref. [19].

$$q(\Omega) = Z_\Omega - N(\Omega), \quad N(\Omega) = \int_\Omega \rho(\mathbf{r})d\tau.$$

This method allows one an exhaustive partitioning of the molecules into the respective atoms, leading to the additivity and transferability of it's properties [21].

The calculation of the electrostatic potential (ESP) was performed using the program *XDPROP*. It can be calculated by the evaluation of

$$V(\mathbf{r}) = \sum_A \frac{Z_A}{|\mathbf{R}_A - \mathbf{r}|} - \int \frac{\rho(\mathbf{r}')d\mathbf{r}'}{|\mathbf{r}' - \mathbf{r}|}$$

where Z_A is the charge on nucleus A located at $\mathbf{R}_A$. The construction assembles positive charges at the nuclei and a continuous distribution of electrons. The calculations were performed based on the isolated from the crystal β-estradiol molecule.

Results and Discussion

Packing

The molecular structure and hydrogen bonding pattern were found to be the same as described by Duax [8]. The packing of this structure results in a formation of six hydrogen bonds ranging in donor-acceptor length from 2.64 – 3.10 Å, these are listed in Table 2. The O(1) atom acts as an acceptor in two hydrogen bonds with hydrogens of two independent urea molecules (H(1NB) and H(2NB)). The H··O vectors of these hydrogen bonds are pointed almost directly at the positions of the lone pairs of O(1). The O(2) atom has a very similar hydrogen bonding structure to O(1) in which it acts as an acceptor in two hydrogen bonds and a donator in one. The hydrogen atoms from the O(1) atom of another independent E_2 molecule and H(2NB) of a urea molecule line up almost directly with the lone pair positions of O(2). Topological analysis yielded in a (3,-1) critical point and a bond path[†] for each hydrogen – acceptor interaction, verifying the true bonding interaction in these hydrogen bonds [22]. The complete table of results from hydrogen bond topology is deposited.

[†] Bond path is a line along which the electron density decreases for any lateral displacement.

Table 2. The geometrical information for the hydrogen bonds.

D—H··A	d (D··A), Å	∠DHA, °
O(2)—H(2O)· ·O(3)	2.6395(7)	169.1(16)
O(1)—H(1O)· ·O(2)	2.6698(7)	171.0(20)
N(1)—H(1NA)· ·O(3)	2.8231(10)	168.6(18)
N(1)—H(1NB)· ·O(1)	2.9783(9)	135.2(16)
N(2)—H(2NB)· ·O(1)	3.0086(9)	161.1(17)
N(2)—H(2NA)· ·O(2)	3.1023(8)	169.1(16)

Kappa Parameters

The coefficients of expansion/contraction of the spherical valence and deformation densities, κ and κ' parameters respectively, are shown in Table 3. The grouping of individual atoms were based on the atom type, hybridization and chemical environment. A total of twelve kappa sets were utilized in order to allow the necessary flexibility while attempting to maintain a minimum number of parameters. As mentioned earlier, the hydrogen atom kappa values were fixed at 1.20. All other kappa values were allowed to refine during the least squares minimization.

Table 3. The expansion/contraction (κ and κ')parameters for the 17β-estradiol•urea crystal

Atoms	Kappa	κ	κ'
O(1), O(2)	1	0.971	0.854
C(3)	2	1.009	0.879
C(17)	3	1.012	0.933
C(1), C(2), C(4)	4	0.976	0.896
C(5), C(10)	5	0.986	0.838
C(6), C(7), C(8), C(9), C(11), C(12), C(13), C(14), C(15), C(16), C(17), C(18)	6	0.985	0.878
all C – H hydrogen atoms	7	1.200	1.200

H(1O), H(2O)	8	1.200	1.200
C(19)	9	0.986	0.818
O(3)	10	0.991	1.080
N(1), N(2)	11	0.996	1.004
all N – H hydrogen atoms	12	1.200	1.200

Atomic Charges

The net atomic charges were derived directly from the monopole populations of the multipole model, as well as from integrating of the electron density within the atomic basins as described by the AIM theory. A complete list of atomic charges determined by both methods are listed in Table 4.

As mentioned earlier, the urea molecule gives us the opportunity to compare our results with previous theoretical and experimental results [6-7]. The atomic charges derived directly from the monopole populations of the multipole model compared favorably to the experimental values reported[‡] by Zavodnik et al. [6], with values matching within one e.s.d. Bader's charges are in a fair agreement with those reported by Gatti et al. [7]. Generally, Bader's charges are significantly bigger than the charges derived from the monopole populations; this is not surprising due to the different ways of calculations. Upon first inspection, a charge of +2.13 e^- for the central carbon seems tremendously high. At the same time, there is evidence in the literature, from both theoretical and experimental data, that this is not unreasonable for a carbon surrounded by electronegative oxygen and nitrogen atoms [7, 23].

The net atomic charges for the atoms of the estrogen molecule derived from the monopole populations of the multipole model were as expected for the given atom types and their chemical neighbors. In addition, like atoms with similar chemical environments exhibited very consistent monopole populations. Again, the charge integrations over atomic basins yielded much greater charges for the oxygen atoms and the atoms directly bound to them, maintaining the consistency between chemically equivalent atoms.

Table 4. Net atomic charges for the atoms of 17β-estradiol • urea

[‡] See the deposition material of Zavodnik et al. (1999) *Acta Crystallogr.* **B55**, 45-54.

Atom	$q(P_v)$	$q(\Omega)$	Atom	$q(P_v)$	$q(\Omega)$
O(1)	-0.534(9)	-1.24	H(1O)	0.401(9)	0.68
O(2)	-0.527(9)	-1.11	H(2O)	0.391(9)	0.67
C(1)	-0.233(16)	-0.19	H(1)	0.206(10)	0.14
C(2)	-0.227(16)	-0.12	H(2)	0.248(9)	0.20
C(3)	0.148(14)	0.49	H(4)	0.249(9)	0.21
C(4)	-0.267(15)	-0.21	H(6A)	0.147(7)	0.15
C(5)	-0.110(15)	-0.09	H(6B)	0.147(7)	0.16
C(6)	-0.265(16)	-0.28	H(7A)	0.146(7)	0.08
C(7)	-0.279(16)	-0.15	H(7B)	0.146(7)	0.10
C(8)	-0.121(14)	-0.12	H(8)	0.180(9)	0.16
C(9)	-0.131(15)	-0.07	H(9)	0.180(9)	0.09
C(10)	-0.106(15)	-0.05	H(11A)	0.147(7)	0.08
C(11)	-0.277(15)	-0.16	H(11B)	0.147(7)	0.09
C(12)	-0.273(15)	-0.14	H(12A)	0.141(7)	0.07
C(13)	-0.158(16)	-0.08	H(12B)	0.141(7)	0.06
C(14)	-0.111(14)	-0.04	H(14)	0.176(8)	0.11
C(15)	-0.294(15)	-0.23	H(15A)	0.141(7)	0.10
C(16)	-0.273(16)	-0.18	H(15B)	0.141(7)	0.13
C(17)	0.168(13)	0.36	H(16A)	0.146(7)	0.11
C(18)	-0.402(17)	-0.24	H(16B)	0.146(7)	0.14
O(3)	-0.234(9)	-1.27	H(17)	0.120(9)	0.14
N(1)	-0.282(12)	-1.41	H(18A)	0.122(6)	0.06
N(2)	-0.286(11)	-1.40	H(18B)	0.122(6)	0.06
C(19)	-0.030(14)	2.13	H(18C)	0.122(6)	0.06
			H(1NA)	0.205(10)	0.49
			H(1NB)	0.209(11)	0.49
			H(2NA)	0.207(10)	0.47
			H(2NB)	0.208(10)	0.49

$q(P_v)$ – net atomic charges derived directly from the monopole populations of the multipole model;
$q(\Omega)$ – Bader's net atomic charges

Topological Analysis

a) urea molecule

Overall values of the electron density at the bond critical points are in a fair agreement with those reported by Zavodnik et al. [6] and Gatti et al. [7], with the exception of the N – H bonds (Table 5). Zavodnik et al. [6] reported significant differences (~0.5 eÅ^{-3}) between the theoretical and experimental electron densities at the (3,-1) critical point for the N – H bond of the urea molecule. The $\rho(r)$ values in this study are much closer to the theoretical values. The difference in the Laplacian values at (3,-1) critical points between experimental and theoretical values is much bigger, showing the sensitivity of the electron density curvature to the different approaches of it's estimation, including the deficiency of the multipole model [24].

Table 5. Topological analysis for the urea molecule.

	this work		Zavodnik, et al. [6]				Gatti, et al. [7]	
	experiment		*experiment*		*theory*		*theory*	
bond	$\rho(r)$	$\nabla^2\rho(r)$	$\rho(r)$	$\nabla^2\rho(r)$	$\rho(r)$	$\nabla^2\rho(r)$	$\rho(r)$	$\nabla^2\rho(r)$
C-O	2.79	-33.15	2.54	-18.86	2.57	-7.92	2.57	-7.95
$(C\text{-}N)_{average}$	2.26	-24.20	2.54	-37.66	2.35	-27.61	2.36	-27.71
$(N\text{-}H)_{average}$	2.22	-28.91	1.82	-31.91	2.34	-47.06	2.34	-47.23

The units for the electron density, $\rho(r)$, are eÅ^{-3}, and for the Laplacian, $\nabla^2\rho(r)$, they are eÅ^{-5}.

A critical point search was also performed in the Laplacian to find the charge density concentration associated with the lone pairs on the urea oxygen. The critical points are (3,+3) in type indicating that $\nabla^2\rho(r)$ is a local minimum at r_c. The critical point information, as well as a plot of the Laplacian in the plane of the lone pairs of the O(3) atom can be seen Table 6 and Fig. 2 respectively. The angle between the lone pairs, being greater that 140°, is much larger than the ideal trigonal planar geometry in agreement with VESPR theory. The inconsistency between the C(3) – O(1) – LP angles are most likely due to the shallow curved shape of the Laplacian in the lone pair region. An extremely small change in $\nabla^2\rho(\mathbf{r})$ could easily move the critical point by 5 – 10°. Gatti et al. [7] also found two (3,+3) critical points in the Laplacian, corresponding to the urea oxygen lone pairs. Although one of their points is very similar to those in Table 6, having the $\nabla^2\rho_c(\mathbf{r}) \cong$ -137 eÅ^{-5} and the O(1)-LP distance of ~0.339 Å, another (3,+3) point is significantly away from the oxygen nucleus (~0.383 Å) having much lower value of the Laplacian (~ -48 eÅ^{-5}). As it has been shown before, the Laplacian values (and it's curvatures) are very 'method-sensitive'.

Table 6. Lone pair Laplacian critical point information for the O(3) atom.

Atom	Lone Pair	$\nabla^2\rho(\mathbf{r}_c)$ ($e\text{Å}^{-5}$)	CP Type	O(1)-LP (Å)	LP1-O(1)-LP2 (°)	C3-O(1)-LP (°)
O(3)	LP1	-149	(3,+3)	0.337	144	118
	LP2	-148	(3,+3)	0.336	144	92

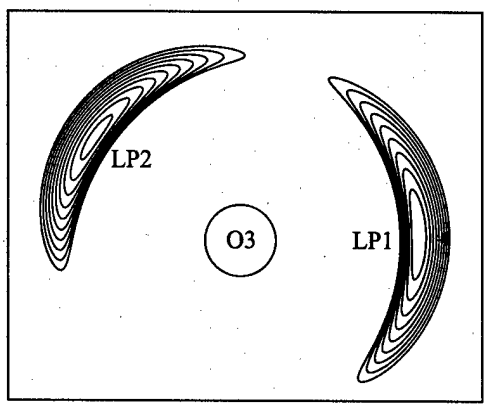

Figure 2. The negative part of the Laplacian in the plane of the O(3) atom lone pairs. Contour interval is -5 $e\text{Å}^{-5}$ starting at -100 $e\text{Å}^{-5}$.

b) E_2 molecule

The critical point analysis of covalent bonds of the estrogen molecule demonstrated the characteristic (3,-1) critical points, with expected $\rho(\mathbf{r}_c)$, $\nabla^2\rho(\mathbf{r}_c)$, and ellipticity values given the hybridization and connectivity. The complete list of all bond critical point properties is deposited. The average $\rho(\mathbf{r}_c)$ values are 1.91 $e\text{Å}^{-3}$ for the C – O bond, 2.17 $e\text{Å}^{-3}$ for C_{ar} – C_{ar}, 1.66 $e\text{Å}^{-3}$ for C – C, 1.91 $e\text{Å}^{-3}$ for C – H and 2.07 $e\text{Å}^{-3}$ for the O – H bond. The critical points are well centered in the homonuclear C – C bonds, and proportionally displaced away from the more electronegative atom in the heteronuclear bonds.

Critical points in the Laplacian corresponding to the lone pairs of both hydroxy oxygen atoms are of the special interest. Table 7 indicates the positions of the lone pair critical points in the Laplacian. The deformation electron density map of the lone pairs of the oxygen O(1), bound to the aromatic ring is presented in Fig. 3, while plot of the Laplacian in the plane of the lone pairs of the O(2) atom is shown in Fig. 4. The finding of two distinct lone pair regions after the

multipole refinement for O(1) was somewhat surprising. We expected that the aromatic hydroxy group, in which hydrogen lies in the plane of the aromatic ring, would be of sp^2 type geometry having some interaction with the π- orbitals of the aromatic ring (the same as in phenol), however, the results of this study indicate that this is not the ground state configuration in the estrogen molecule. The distances of the lone pairs from the oxygen atoms are very consistent. This is believed to be at least partially to due to the fact that the contraction/expansion coefficients for both oxygen atoms are constrained to be equal. Same as in the urea molecule, the angles between the lone pairs agree with VESPR theory in that they are much larger than the ideal tetrahedral value.

Table 7. Lone pair Laplacian critical point information for the O(1) and O(2) atoms.

Atom	Lone Pair	$\nabla^2\rho(\mathbf{r}_c)$ (eÅ^{-5})	O-LP (Å)	LP1-O-LP2 (°)	C-O-LP (°)	H-O-LP (°)
O(1)	LP3	-133	0.346	146	104	103
	LP4	-119	0.347	146	90	100
O(2)	LP5	-129	0.346	235	108	115
	LP6	-120	0.346	235	88	101

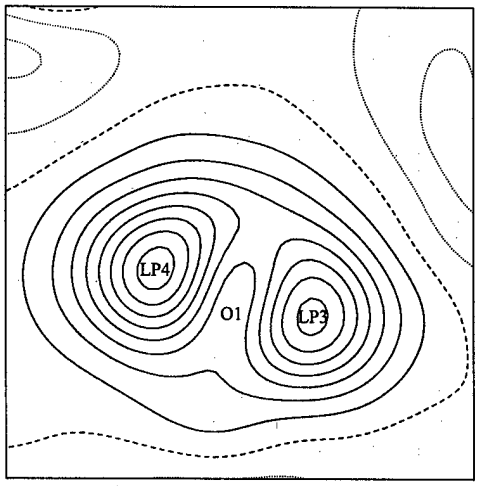

Figure 3. Dynamic model deformation density map in the plane of the lone pairs of the O(1) atom. Contour intervals are 0.05 eÅ^{-3} with solid lines positive, dashed lines zero, and dotted lines negative.

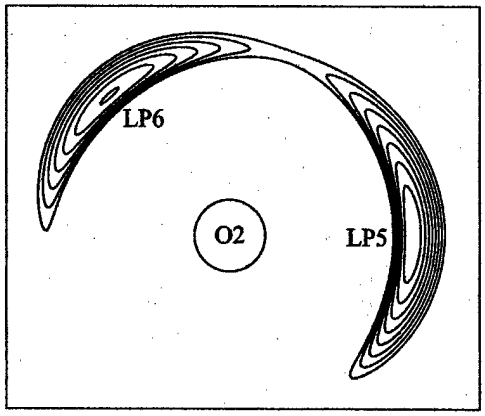

Figure 4. The negative part of the Laplacian in the plane of the lone pairs of the O(2) atom. Contour intervals are -5 $eÅ^{-5}$ starting at -80 $eÅ^{-5}$.

Electrostatic Potential

The core structure of the estrogen molecule generally is hydrophobic and relatively predictable in terms of the electrostatic potential. The ESP plotted on the van der Waals molecular surface for the E_2 molecule with the program package *MOLMOL* [25] is shown in Fig. 6. Since the isolated molecule (taken from the crystal) is calculated in this case, the ESP does not reflect the interactions in the condensed phase, such as hydrogen bonding. The negative potential areas (red) are produced by the aromatic ring, oxygens and some of carbon atoms (Fig. 6), while the hydrogen atoms involved in the hydrogen bonding produce highly positive areas (blue) on the molecular surface.

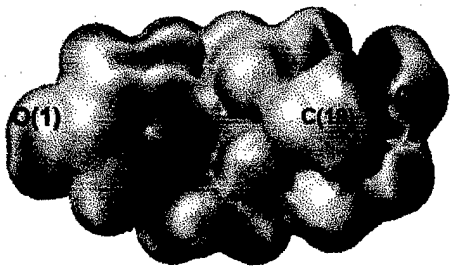

Figure 6. The E_2 electrostatic potential plotted on the van der Waals molecular surface. Negative values are in red, positive are in blue.

The hydroxy groups are of particular interest in the E_2 molecule, offering varying environments being bound to sp^2 and sp^3 type carbons and being involved in several hydrogen

bonds. The consistency in the lone pair density, in shape, size, position, and hydrogen bonding geometry suggested that the electrostatic potential surrounding the oxygen atoms might be relatively consistent in shape and magnitude. This however was not the case. Fig. 7 demonstrates the electrostatic potential of the O(1) hydroxy group lone pair region. The significant portion of the negative ESP extends approximately 180° around the oxygen. A maximum ESP of ~ -0.20 $eÅ^{-1}$ was observed for this hydroxy group. The additional negative regions displayed represent the potential created by the π density of the aromatic ring. The oxygen atom forms a continuum with the negative potential above and below the aromatic ring.

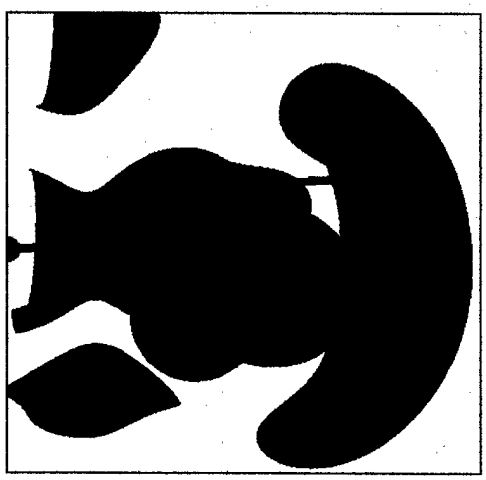

Figure 7. Electrostatic potential isosurface around the O(1) atom. The blue surface represents +1.0 $eÅ^{-1}$, while the red surfaces represent –0.15 $eÅ^{-1}$.

Before discussing the O(2) hydroxy group, it is important to recognize the orientation of the hydrogen atom H(2O). A hydroxy group attached to an aromatic ring almost exclusively has the hydrogen atom in the plane of the ring. Obviously, a hydroxy group bound to an sp^3 carbon can freely rotate. In the solid state, the orientation of the OH group will almost always be defined by the hydrogen bonding scheme. Fig. 8 displays the D-ring[§] of the E_2 molecule and the torsion angle (γ) of 49° between H(2O) and H(17).

[§] The C(13)-C(14)-C(15)-C(16)-C(17) ring.

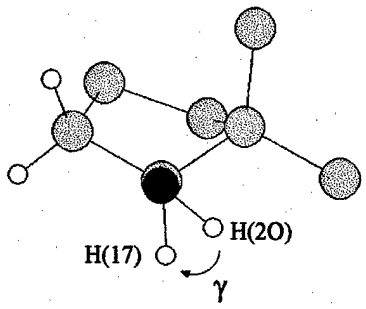

Figure 8. The O(2) hydroxy group geometry showing torsion angle (γ) between the H(2O) and H(17) atoms. The O(2) atom is shown in red.

The negative electrostatic potential around O(2) has much greater maximum value than that of the O(1) hydroxy group, reaching a value of ~ -0.35 eÅ^{-1}. In addition, the ESP does not evenly cover the lone pair region as on the O(1) hydroxy group. A shift toward the lone pair opposite H(17) appears to have taken place (Fig. 9). The coverage area of the negative potential seems smaller, covering near 120°, versus the approximate 180° coverage on O(1).

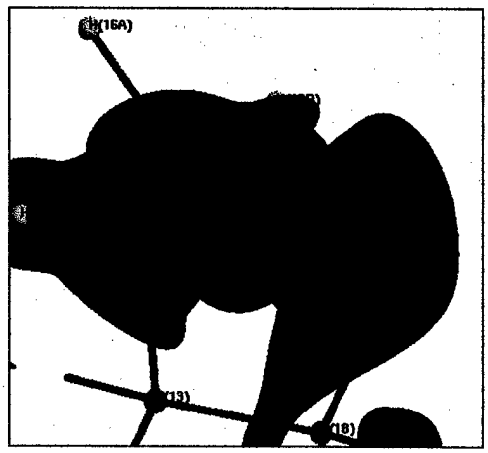

Figure 9. Electrostatic potential isosurface around the O(2) atom. The blue surface represents +1.0 eÅ^{-1}, while the red surfaces represent –0.25 eÅ^{-1}.

It is believed that the agonistic or the antagonistic responses of different estrogens can be related to their electrostatic potential [3]. We intend to construct a database with ESP calculated for estrogens with different biological activities. Once enough data are available, we hope to identify specific topological features in these estrogens that distinguish binding ability of these molecules to the estrogen receptor.

Conclusions

This is one of the first charge density studies accomplished for the big (56 atoms) organic molecules in the non-centrosymmetric unit cell. Our study showed that it is possible to get a quality data for such kind of system; the optimal coordinate system and slow, initially constrained refinement are the necessary tools for this type of study. Since most estrogens are identical in the core structure of the molecule, this study will provide a better starting point for future multipole refinements of other estrogen derivatives. Overall our results pertaining to the urea molecule reasonably agree with the previous literature results showing the quality of our data.

For the E_2 molecule, the lone pair densities of the oxygen atoms, which are an extremely small features of the system, were found to be quite similar. This indicates that the oxygen atom bound at the C(3) position do not have a strong interaction with the π orbitals of the aromatic ring in the ground state configuration. Despite this consistency, the electrostatic potentials in the region of the hydroxy groups differ greatly in both shape and magnitude. Future studies may reveal how the H(17) – C(17) – O(2) – H(20) torsion angle affects the electrostatic potential of the C(17) hydroxy group. Obviously many more estrogen systems must be completed before the comparative portion of the study can take place and real conclusions can be made on the relationship between the electrostatic potential and estrogenic action.

We would like to thank Dr. Samuel Brooks for his contribution. We thank Dr. A.Volkov and Prof. P. Coppens for making *TOPXD* program available for us. We would also like to thank the Department of Defense for their financial support (Grant # DAMD17-00-1-0468).

Supplemental Tables and figures

S1 – experimental protocol

S2 - atomic coordinates

S3, S4 - atomic thermal parameters

S5 - bond lengths

S6 - bond angles

S7,S8,S9 – multipole populations

S10, S11,S12 - topological results

Fig. D1. Local multipole coordinate system for the urea molecule

1. Korach, K.S. (1994) *Science*. **266**, 1524-1527.
2. Lacassagne, A. (1936) *American Journal of Cancer*. **27**, 217-225.
3. VanderKuur, J.A., Wiese, T. & Brooks, S.C. (1993) *Biochemistry*. **32**, 7002-7008.
4. Gutendorf, B. and Westendorf, J. (2001) *Toxicology*. **166**, 79-89.
5. Nishihara, T., Nishikawa, J., Kanayama, T., Dakeyama, F., Saito, K., Imagawa, M., Takatori, S., Kitagawa, Y., Hori, S. & Utsumi, H. (2000) *Journal of Health Science*. **46**, 282-298.
6. Zavodnik, V., Stash, A., Tsirelson, V., De Vries, R. & Feil, D. (1999) *Acta Crystallographica*. **B55**, 45-54.
7. Gatti, C., Saunders, V.R. & Roetti, C. (1994) *Journal of Chemical Physics*. **101**, 10686-10696.
8. Duax, W.L., (1972) *Acta Crystallographica*. **B28**, 1864-1871.
9. BRUKER-AXS, *SAINT Software Package*. 1999, Madison, Wisconsin.
10. Kirschbaum, K., Martin, A. & Pinkerton, A.A. (1997) *Journal of Applied Crystallography*. **30**, 514-516.
11. Blessing, R.H., (1997) *Journal of Applied Crystallography*. **30**, 421-426.
12. Sheldrick, G.M. (1997) *SHELXL-97: Program for Crystal Structure Refinement* (University of Gottingen, Gottingen, Germany).
13. Koritsanszky, T., Howard, S., Mallison, P.R., Su, Z., Richter, T., & Hansen, N.K. (1995) *XD. A Computer Program Package for Mulitpole Refienement and Analysis of Electron Densities from Diffraction Data* (Berlin).
14. Hansen, N. & Coppens, P. (1978) *Acta Crystallographica*. **A34,** 909-921.
15. Chen, Yu.-Sh., Kirschbaum, K., Parrish, D., Pinkerton, A.A., Poomani, K. & Zhurova, E.A. (2003) *Journal of Applied Crystallography* (submitted).
16. Coppens, P., Guru Row, T.N., Leung, P., Stevens, E.D., Becker, P.J. & Yang, Y.W. (1979) *Acta Crystallographica*. **A35**, 63-72.
17. Coppens, P. (1997) *X-Ray Charge Densities and Chemical Bonding* (New York: Oxford University Press).
18. Volkov, A., Abramov, Y.A. & Coppens, P. (2001) *Acta Crystallographica*. **A57,** 272-282.

19. Bader, R.F.W. (1990) *Atoms in Molecules : A Quantum Theory* (Oxford: Oxford University Press).

20. Volkov, A., Gatti, C., Abramov, Yu. & Coppens, P. (2000) *Acta Crystallographica.* **A56**, 252-258.

21. Bader, R.F.W. (1994) *Physical review.* **B49**, 13348-13356.

22. Bader, R.W.F. (1998) *Journal of Physical Chemistry* **A102**, 7314-7323.

23. Li, X., Wu, G., Abramov, Y.A., Volkov, A.V. & Coppens, P. (2002) *Proceedings of the National Academy of Sciences of the United States of America.* **99**, 12132-12137.

24. Volkov, A., Abramov, Yu., Coppens, P. & Gatti C. (2000) *Acta Crystallographica.* **A56**, 332-339.

25. Koradi, R., Billeter, M. & Wüthrich, K. (1996) *Journal of Molecular Graphics.* **14**, 51-55.